



**FEEDBACK LINEARIZATION CONTROL OF FLEXIBLE JOINT PARALLEL
MANIPULATORS BY SOLVING SINGULAR ACCELERATION LEVEL
DIFFERENTIAL EQUATIONS**

HARITH ABDALJAWAD

JUNE 2016

**FEEDBACK LINEARIZATION CONTROL OF FLEXIBLE JOINT PARALLEL
MANIPULATORS BY SOLVING SINGULAR ACCELERATION LEVEL
DIFFERENTIAL EQUATIONS**

A THESIS IS SUBMITTED TO

THE GRADUATE SCHOOL OF NATURAL AND APPLIED SCIENCES OF

ÇANKAYA UNIVERSITY

BY

HARITH ABDALJAWAD


**IN PARTIAL FULLFILMENT OF THE REQUIREMENTS
FOR
THE DEGREE OF MASTER OF SCIENCE
IN
MECHANICAL ENGINEERING**

JUNE 2016

Title of the Thesis : **FEEDBACK LINEARIZATION CONTROL OF FLEXIBLE JOINT PARALLEL MANIPULATORS BY SOLVING SINGULAR ACCELERATION LEVEL DIFFERENTIAL EQUATIONS**

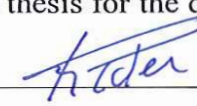
Submitted by **Harith ABALJAWAD**

Approval of the Graduate School of Natural and Applied Sciences, Çankaya University.



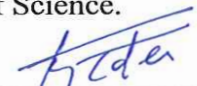
Prof. Dr. Halil Tanyer EYYUBOĞLU
Director

I certify that this thesis satisfies all the requirements as a thesis for the degree of Master of Science.



Prof. Dr. S. Kemal İder
Head of Department

This is to certify that we have read this thesis and that in our opinion it is fully adequate, in scope and quality, as a thesis for the degree of Master of Science.



Prof. Dr. Kemal İder
Supervisor


Examination Date: 01.06.2016


Examining Committee Members


Prof. Dr. S. Kemal İder (Çankaya Univ.)

Asst. Prof. Dr. Özgün SELVİ (Çankaya Univ.)

Assoc. Prof. Dr. Fahd JARAD (T.H.K Univ.)







STATEMENT OF NON-PLAGIARISM PAGE

I hereby declare that all information in this document has been obtained and presented in accordance with academic rules and ethical conduct. I also declare that, as required by these rules and conduct, I have fully cited and referenced all material and results that are not original to this work.

Name, Last Name : ABDALJAWAD, Harith

Signature : 

Date : 01.06.2016

ABSTRACT

FEEDBACK LINEARIZATION CONTROL OF FLEXIBLE JOINT PARALLEL MANIPULATORS BY SOLVING SINGULAR ACCELERATION LEVEL DIFFERENTIAL EQUATIONS

ABDALJAWAD, Harith

M.Sc., Department of Mechanical Engineering

Supervisor: Prof. Dr. S. Kemal İder

June 2016, 61 pages

This study utilizes a certain algorithm where joint drives flexibility is presented for solving singular set of differential equations by specified implicit numerical integration method that is called Backward Euler Formula for more advanced order derivative information. The reason for using such a procedure is that there is singularity presence at the acceleration level inverse dynamics equations because the control torques can't perpetuate a direct effectiveness at the end-effector accelerations as a result of the elastic media. The trajectory tracking control law is utilized for a 3R (revolute joint), three legs planar parallel manipulator. This law linearizes and decouples the system which leads to achieve asymptotic stability by the means of feeding back the positions and velocities of the actuated rotors and joints. The desired path of the end-effector is chosen for the sake of singularity avoidance.

Keywords: Parallel manipulator, flexible joint, inverse dynamics control

ÖZ

**SİNGÜLER İVME SEVİYESİNDEKİ DİFERANSİYEL DENKLEMLERİ
ÇÖZMEK SURETİYLE ESNEK MAFSALLI PARALEL
MANİPÜLATÖRLERİN KONTROLÜ**

ABDALJAWAD, Harith

Yüksek Lisans, Makine Mühendisliği Anabilim Dalı

Tez Yöneticisi: Prof. Dr. S. Kemal İder

Haziran 2016, 61 sayfa

Esnek mafsallı robot manipülatörlerde elastik ortamdan dolayı kontrol torkları ile uç işlemci ivmesi anlık ilişkili değildir. Bu sebeple ivme seviyesindeki ters dinamik denklemleri singüler bir diferansiyel denklem sistemi (diferansiyel/cebirsal denklem sistemi) oluşturur. Bu tezde bu denklemler bir dolaylı (implicit) nümerik integrasyon yöntemi olan geri Euler yöntemi ile çözümlenerek sistemin hareket kontrolü yapılmaktadır. Yörünge kontrolünün sağlandığı kontrol kanunu her birinde üç döner mafsallı bulunan üç ayaklı ve üç serbestlik dereceli bir düzlemsel paralel manipülatöre uygulanmıştır. Mafsalların ve aktüatör rotorlarının açısal konumlarını ve açısal hızlarını geri besleyerek asimptotik stabilite elde edilmiştir.

Anahtar Kelimeler: Paralel manipölator, esnek eklem, ters dinamik kontrol.



AKNOWLEDGMENTS

I would like to declare my gratitude to my supervisor Prof. Dr. Kemal İder for the science that he gave to me with full generosity and support.

My mother, the flower of my life, my father's soul and all my friends who supported me, thank you all.

My childhood friend Naseem Al-TALIBI, rest in peace brother.

TABLE OF CONTENTS

STATEMENT OF NON PLAGIARISM	iii
ABSTRACT	iv
ÖZ	v
ACKNOWLEDGEMENTS	vii
TABLE OF CONTENTS.....	viii
LIST OF FIGURES	x
LIST OF TABLES	xii

CHAPTERS:

1.	INTRODUCTION.....	1
	1.1. Literature Review.....	1
	1.2. Purpose of Study.....	4
	1.3. Outline of the Study.....	4
2.	ROBOT DYNAMICS AND CONTROL.....	5
	2.1 Preview.....	5
	2.2 Robot Dynamics.....	7
	2.3 System Equations of Motion.....	8

2.5.1	Task Space Equation.....	12
2.5.2	Control Law.....	16
2.5.3	Position Error Dynamics.....	21
3.	THREE REVOLUTE JOINTS THREE LEGS PLANAR PARALLEL ROBOT STUDY AND SIMULATION.....	22
3.1	Planar Parallel Robot Study.....	22
3.1.1	Kinetic Energy.....	26
3.1.2	Potential Energy.....	34
3.1.3	Closed-Loop Constraint Equations.....	36
3.1.4	System Equations of Motion.....	40
3.2	Control Simulation and Results.....	44
4.	DISCUSSIONS AND CONCLUSION.....	59
4.1	DISCUSSIONS.....	59
4.2	CONCLUSION.....	60
	REFERENCES.....	61
	APPENDECIES.....	A1
	A. CURRICULUM VITAE.....	A1

LIST OF FIGURES

FIGURES

Figure 1	Flexible Joint Dynamic Model.....	6
Figure 2	3-RRR Planar Parallel Robot Architecture.....	23
Figure 3	3-RRR Planar Parallel Robot.....	24
Figure 4	Three Open Kinematic Chains.....	25
Figure 5	Position Response 1. x_1 , 2. x_2 , 3. x_3 (First Group $\omega_0 = 20rad/s$).....	48
Figure 6	Position Response 1. x_1 , 2. x_2 , 3. x_3 (First Group $\omega_0 = 30rad/s$).....	48
Figure 7	Control Torques 1. T_1^a , 2. T_2^a , 3. T_3^a (First Group $\omega_0 = 20 rad/s$).....	49
Figure 8	Control Torques 1. T_1^a , 2. T_2^a , 3. T_3^a (First Group $\omega_0 = 30 rad/s$).....	49
Figure 9	Deflections 1. $\theta_1 - \phi_1$, 2. $\theta_2 - \phi_2$, 3. $\theta_3 - \phi_3$ (First Group $\omega_0 = 20rad/s$).....	50
Figure 10	Deflections 1. $\theta_1 - \phi_1$, 2. $\theta_2 - \phi_2$, 3. $\theta_3 - \phi_3$ (First Group $\omega_0 = 30rad/s$).....	50
Figure 11	Position Response 1. x_1 , 2. x_2 , 3. x_3 (Second Group $\omega_0 = 20rad/s$).....	51
Figure 12	Position Response 1. x_1 , 2. x_2 , 3. x_3 (Second Group $\omega_0 = 30rad/s$).....	51
Figure 13	Control Torques 1. T_1^a , 2. T_2^a , 3. T_3^a (Second Group $\omega_0 = 20 rad/s$).....	52

Figure 14	Control Torques 1. T_1^a , 2. T_2^a , 3. T_3^a (Second Group $\omega_0 = 30 \text{ rad/s}$).....	52
Figure 15	Deflections 1. $\theta_1 - \phi_1$, 2. $\theta_2 - \phi_2$, 3. $\theta_3 - \phi_3$ (Second Group $\omega_0 = 20 \text{ rad/s}$).....	53
Figure 16	Deflections 1. $\theta_1 - \phi_1$, 2. $\theta_2 - \phi_2$, 3. $\theta_3 - \phi_3$ (Second Group $\omega_0 = 30 \text{ rad/s}$).....	53
Figure 17	Position Errors (Second Group $\omega_0 = 20 \text{ rad/s}$).....	54
Figure 18	Position Errors (Second Group $\omega_0 = 30 \text{ rad/s}$).....	54
Figure 19	Position Response 1. x_1 , 2. x_2 , 3. x_3 (Third Group $\omega_0 = 20 \text{ rad/s}$).....	55
Figure 20	Position Response 1. x_1 , 2. x_2 , 3. x_3 (Third Group $\omega_0 = 30 \text{ rad/s}$).....	55
Figure 21	Control Torques 1. T_1^a , 2. T_2^a , 3. T_3^a (Third Group $\omega_0 = 20 \text{ rad/s}$).....	56
Figure 22	Control Torques 1. T_1^a , 2. T_2^a , 3. T_3^a (Third Group $\omega_0 = 30 \text{ rad/s}$).....	56
Figure 23	Deflections 1. $\theta_1 - \phi_1$, 2. $\theta_2 - \phi_2$, 3. $\theta_3 - \phi_3$ (Third Group $\omega_0 = 20 \text{ rad/s}$).....	57
Figure 24	Deflections 1. $\theta_1 - \phi_1$, 2. $\theta_2 - \phi_2$, 3. $\theta_3 - \phi_3$ (Third Group $\omega_0 = 30 \text{ rad/s}$).....	57
Figure 25	Position Errors (Second Group $\omega_0 = 20 \text{ rad/s}$).....	58
Figure 26	Position Errors (Third Group $\omega_0 = 30 \text{ rad/s}$).....	58

LIST OF TABLES

TABLES

Table 1
Table 2

CHAPTER 1

INTRODUCTION

1.1 Literature Review

Parallel manipulators took an interest of research for more than twenty years because of the advantages they have as compared to the serial ones. As a result of the closed loop structure of the parallel manipulators, this made them carry heavier loads. Real time applications like earthquake simulators, flight simulators and micro-motion manipulators are the most known industrial applications for these mechanics where high motion accuracy and high load capacity are needed. Also some problems may take place such as difficulties in the operation of control and also relatively small work space may be exist, as a result parallel manipulators took a lot of interest in different areas of research.

Parallel manipulators gains drive singular positions as well as to the kinematic singular positions which serial robots also have. Singularity analysis of parallel manipulators has been the subject of many studies in the last years.

İder [1] examined the singularities that occur in the parallel manipulators and showed that the manipulator shall pass through the singular positions when the system motion and the actuator forces keeping its' stability by the mean of modifying the system equations of motion.

Joint flexibility must be regarded in the control system because of the latter's importance in control system design and manipulator dynamics, as a result high precision manipulators will be handled.

Serial manipulators flexible joints control was studied by many researchers as well they took interest after the derivation of the flexible joint model done by Spong [2].

Two nonlinear control schemes are put forward among all the motion control methods, those two schemes are called the feedback linearization and singular perturbation approaches.

The singular perturbation process depends on the benefit of the order decreasing by resolving the main system into two subsystems that are known as a fast subsystem and a low subsystem that are the flexible joints and rigid manipulator respectively. By disregarding and then correcting due to the fast phenomena the model will be lowered, the latter will be reintroduced by measuring them separately with different time scales where the slow variables are considered as constant. However this way is said to be valid if and only if the joint springs are stiff in a sufficient way, this will cause the approach to be limited.

Another name of the feedback linearization control of flexible-joints that is the analytical inverse dynamics control which is studied by various authors.

From this method, the intermediate variables are eliminated and the inputs are solved as functions of end-effector motion till the fourth derivative, Moreover, for the elimination it will be necessary to differentiate the motion equations and the task equations at acceleration level twice.

Jankowski and Van Brussel [3] applied inverse dynamics control in discrete time where solution of the singular sets of differential equations are used to avoid further differentiations of the system equations of motion.

Forrest-Barlach and Babcock [4] used the inverse dynamics control method for the cylindrical coordinate arm with drive train compliance and actuator dynamics in the radial and each of the revolute degree of freedom.

İder and Özgören [5] used an acceleration level feedback linearization control the by using implied numerical integration methods that account for the greater order derivatives information for the purpose of solving the set of the singular differential equations. The asymptotic stability is achieved by feeding back the joints positions, velocities and velocities of rotors.

All of the above studies focused on the control of flexible joint serial manipulators. There are limited numbers of studies in the literature concerning control of parallel manipulators. Most of these studies did not take the joint flexibility into their control strategies.

Dado and Al-Huniti [6] studied dynamic simulation approach for a mixed-loop planar manipulators with joint-drive flexibility. The mathematical model of a five-link, three degree of freedom manipulator was derived using the virtual work method. The drive signal at the motor was based on the error between the actual and desired motions by using the suitable gains for position and velocity.

Chablat and Wenger [7] showed that a non-singular robot assembly can that change trajectory is exist for a symmetrical planar robot with triangle platform and equilateral base by presenting the kinematic analysis of a three-degree-of-freedom planar parallel robot. It has been showed that in apposite to serial ones, planar parallel manipulators can pass through multiple direct kinematic solutions together with the multiple inverse kinematic ones, that gives greater flexibility with the trajectory-planning stage.

İder and Korkmaz [8] developed and utilized an inverse dynamics control law for the aim of control of a path tracking of a specified flexible-joint parallel manipulator by further differentiation of the dynamic equations till third and fourth order derivatives, the closed system is converted into an open one by the mean of disconnecting a satisfying number of non-actuated joints, then by eliminating the intermediate variables and the Lagrange multipliers that gives a fourth-order input-output relation, after that and by feeding back the positions and the velocities of the actuated rotors and joints asymptotic stability is achieved.

1.2 Purpose of Study

The purpose behind this thesis is to decide trajectory tracking control of the end effector of the planar parallel manipulator by making use of the feedback linearization [inverse dynamics] approach regarding joint flexibility. To ease the solution and reduce the online computation, singular acceleration stage inverse dynamic equations are solved by implicit numerical integration techniques. By utilizing this previous procedure, further differentiation of the equation of motion, the task equations and the constraint is avoided so as to reduce the complexity of calculations. The presented control strategy gives asymptotic stability while testing the trajectory tracking control of the end-effector motion. On the other hand additional complexity will be avoided by neglecting the effect of the viscous friction at the passive joints, the rotor damping characteristic and the structural damping of the active joints.

1.3 Outline of the Study

The following chapters are organized in this thesis in order to demonstrate the control algorithm and the case study.

Chapter 2, is related to the dynamics of the parallel manipulator that are explained when the joint flexibility is regarded into the analysis. The system constraint equations and system equations of motion are derived, as well the feedback linearization control approach is considered. The task space equations and the control law are introduced. The execution for the elimination of the non-actuated joint variables from the system constraint equations and the elimination of actuator variables off the equations of motion are considered so as to get the input/output relation.

In Chapter 3, the dynamic equations of 3RRR planar parallel manipulator with flexibility at the actuated joints are derived, its' control law is formulated and numerical simulations are made.

Chapter 4, discusses and concludes the similes of the simulations.

CHAPTER 2

ROBOT DYNAMICS AND CONTROL

2.1 Preview

Let the system of an n degree of freedom parallel manipulator be changed into an open-tree structure by the mean of separating a suitable number of non-actuated joints, and the degree of freedom of that system is m , i.e., in the parallel manipulator the number of independent loop closure constraints be $m-n$. The set of the generalized coordinates corresponding to the robot joint variables that express the relative joint positions assumed to be defined as $\{\theta_1, \dots, \theta_m\}$.

So that the vector belongs to the manipulator joint variables of the rigid links which contains both of the actuated and non-actuated joints is

$$\bar{\theta} = [\theta_1, \dots, \theta_m]^T \quad (2.1)$$

By separating the joint coordinate vector into two sub-vectors that corresponded to the variables of the actuated joints and the non-actuated joints respectively \bar{q} ($n \times 1$), $\bar{\theta}^u$ [$(m - n) \times 1$], such that, $\bar{\theta}^T = [\bar{q}^T \quad \bar{\theta}^{uT}]$.

The degree of freedom of any parallel manipulator decides the number of the actuated joints of that manipulator. Joints elasticity occurs at the actuated joints as a result of the

elasticity of the transmissions. The elasticity sources at the joints are mainly harmonic drives and thin shafts used in drive trains, couplings. It is important to take joint flexibility into consideration so as to gain higher performance from the controller since joint flexibility is the main source as compared to the total manipulator flexibility as practically verified by Rivin [9].

At an actuated joint, Joint elasticity of the power transmission elements is modeled as a torsional spring, on the other hand, structural damping is neglected.

For the i^{th} transmission, K_i stand for the spring constant as shown in figure 2.1.

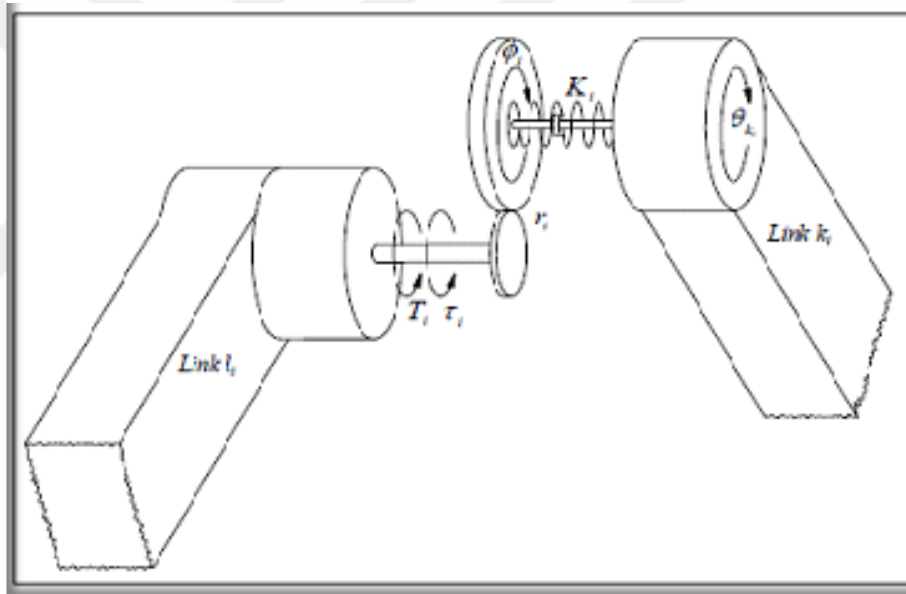


Figure 1 Flexible Joint Dynamic Model

The figure above refers to the i^{th} transmission, where θ_{k_i} represent the robot joint variable that corresponds to the driven links' angular position (k_i) with regard to the link (l_i) where the i^{th} actuator is mounted.

Moreover, in the above flexible model, τ_i represents the actuator position of the i^{th} actuator with regard to the link where the actuator mounted. ϕ_i represents the actuator variable that may be given by the following formula

$$\phi_i = \tau_i/r_i \quad i = 1, \dots, n \quad (2.2)$$

where r_i stands for the speed reduction ratio.

On the other hand, the set of the generalized coordinates refers to the actuator variables are

$$\{\phi_1, \dots, \phi_n\}$$

As a result, actuator joint variables of the robot may be given by the vector

$$\bar{\phi} = [\phi_1, \dots, \phi_n]^T \quad (2.3)$$

K_i stands for the spring constant of the i^{th} transmission.

2.2 Robot Dynamics

The equations of motion will be simplified and so as to make them more suitable for the control and analysis, this will be done by using some assumptions stated by [2], the assumptions are as below:

- The rotor/gear inertia is symmetric about the axis of rotation of the rotor as a result the velocity of the rotor center of mass and the gravitational potential of the system become independent of the rotor position.
- The links of the robot are rigid.
- By choosing a large enough gear ratio, as a result, the rotor kinetic energy will be generally due to its own rotation.

The formula $1/2[I_i^r(\omega_z + r_i\dot{\phi}_i)^2 + I_i^{r*}(\omega_x^2 + \omega_y^2)]$ represents the rotational kinetic energy of the i^{th} actuator, where I_i^r stands for the i^{th} rotor moment of inertia about its

rotational axis and I_i^{r*} stands for the moment of inertia of the cylindrical rotor about the axes that are perpendicular to the rotation axis through the center of mass.

The angular velocity components $\omega_x, \omega_y, \omega_z$ of the link that the actuator is placed where the angle of the rotor is mensurationed about the Z-axis.

Since $\dot{\phi}_i$ and $\omega_x, \omega_y, \omega_z$ have the same order of magnitude and if r_i is sufficiently large, as a result, the rotational kinetic energy of the drive is approximately $1/2I_i^r (r_i \dot{\phi}_i)^2$ [8].

Additional degrees of freedom appear because of the elastic transmission between the actuators and the links. As a result, at each actuator the rotor is modeled as a fictional link and so an n degree of freedom is added to the system that makes the general system a 2n degree of freedom system.

To find the equations of motion responding to the two sets of generalized coordinates showed in 2.1 and 2.3, Lagrange's equations are used.

The Lagrange's equation of the first set of the generalized coordinates that correspond to the robot joint variables is shown below

$$\frac{d}{dt} \left(\frac{\partial K}{\partial \dot{\theta}_j} \right) - \frac{\partial K}{\partial \theta_j} + \frac{\partial D}{\partial \dot{\theta}_j} + \frac{\partial U}{\partial \theta_j} = \tilde{Q}_j + Q'_j \quad j=1, \dots, m \quad (2.4)$$

The Lagrange's equation of the second set of the generalized coordinates that correspond to the robot joint variables is shown below

$$\frac{d}{dt} \left(\frac{\partial K}{\partial \dot{\phi}_j} \right) - \frac{\partial K}{\partial \phi_j} + \frac{\partial D}{\partial \dot{\phi}_j} + \frac{\partial U}{\partial \phi_j} = Q''_j \quad j=1, \dots, n \quad (2.5)$$

Where K, D, U, \tilde{Q}_j , Q'_j and Q''_j represent the following terms respectively (kinetic energy, dissipation function, potential energy, generalized contact forces, generalized constraint forces and generalized actuator forces).

D terms are all zeros according to the presented assumptions of neglecting the damping terms.

2.3 System Equations of Motion

According to Spong [2] assumptions given in 2.2, the following equations of motion are presented

$$\hat{M}\ddot{\bar{\theta}} + \bar{Q} + \tilde{K} + \bar{F}^c = 0 \quad (2.6)$$

$$\hat{r}^r \ddot{\bar{\phi}} - \tilde{K}(\bar{q} - \bar{\phi}) = \bar{T} \quad (2.7)$$

where, $\hat{M}(\bar{\theta})$ is the $m \times m$ generalized mass matrix which is positive definite and symmetric and $\bar{Q}(\bar{\theta}, \dot{\bar{\theta}})$ is the $m \times 1$ vector of gravitational, centrifugal and Coriolis terms. \bar{Q} and \hat{M} are the same as those of the open system case, regardless elasticity where the rotors are considered as a part of the identical links.

This is because the terms of the inertia coupling between $\bar{\theta}$ and $\bar{\phi}$ disappeared.

\tilde{K} is an $m \times 1$ vector that contains stiffness terms such a way that

$$\tilde{K} = \begin{bmatrix} \hat{K}(\bar{q} - \bar{\phi}) \\ 0 \end{bmatrix}$$

Where \hat{K} is an $n \times n$ diagonal stiffness matrix with $K_{ii} = k_i, i = 1, \dots, n$.

\hat{r}^r is an $n \times n$ matrix that contains the elements of the inertial parameters of the links and may be expressed as

$$\hat{r}^r = \text{diag}[I_i^r r_i^2] \quad i = 1, \dots, n \quad (2.8)$$

\bar{T} is the $n \times 1$ vector of the control torques after the speed reduction.

\bar{F}^c is the vector of generalized constraint forces due to the closed loop formation. To find F^c loop closure constraint equations must be defined.

$$B\dot{\theta} = 0 \quad (2.9)$$

where $B(\theta)$ is an $(m - n) \times m$ stands for the constraint Jacobian matrix with

$$B_{ij} = \partial q_i / \partial \theta_j, i = 1, \dots, m - n, j = 1, \dots, m.$$

In order to satisfy that the kinetic energy of the rotor is due basically to its' own rotation [1], the gear ratio assumed to be large enough.

As a result, F^c can be defined as

$$\bar{F}^c = \hat{B}^T \bar{\lambda} \quad (2.10)$$

where λ is an $(m - n) \times 1$ stands for the Lagrange multipliers vector.

Kinetic and potential energy terms and all the other terms related to them will be present in chapter 3.

2.4 Closed Loop Constraints

The constraint equations are necessary for the purpose of writing the non-actuated joint coordinate by using the actuated joint coordinate terms.

After the disconnected constraint equations of the robot are written in loop closure form in terms of position, velocity and matrix form as below,

$$q_i(\theta_1, \dots, \theta_m) = 0 \quad (2.11)$$

$$\sum_{j=1}^m B_{ij} \dot{\theta}^j \quad (2.12)$$

$$\hat{B} \dot{\theta} = \bar{0} \quad (2.13)$$

\hat{B} is an $(m - n) \times m$ matrix is now constructed, However there will be two sub-matrices when the terms of the non-actuated joint variables are written in terms of the actuated ones and this shall give an $(m - n) \times n$ \hat{B}^a matrix and $(m - n) \times (m - n)$ matrix \hat{B}^u and equation 2.12 can be written now as below

$$\hat{B}^u \dot{\theta}^u = \hat{B}^a \dot{q} \quad (2.14)$$

$\dot{\theta}^u$ May be found as

$$\hat{C} \dot{q} = \dot{\theta}^u \quad (2.15)$$

$$\hat{C} = -(\hat{B}^u)^{-1} \hat{B}^a \quad (2.16)$$

and

$$\ddot{\theta}^u = \hat{C} \ddot{q} + \dot{\hat{C}} \dot{q} \quad (2.17)$$

and

$$\dot{\hat{C}} = -\left((\dot{\hat{B}}^u) \hat{B}^a + (\hat{B}^u)^{-1} \dot{\hat{B}}^a \right) \quad (2.18)$$

where \hat{C} is an $(m - n) \times n$ matrix.

Further differentiations will not be needed because an implicit numerical integration method will be used for the control scheme.

2.5 Inverse Dynamics Control

2.5.1 Task Space Equations

The control technique used for the robot that has m links and n actuators at the joints is basically depends on finding a connection between the inputs and the outputs. The inputs through the actuating motors can be voltages supplied to those actuators or joint torques/forces. The outputs are the joint positions either in joint space or in task space since the control problem main aim is the end effector position tracking.

A relation must be derived between the joint space and the task space coordinates since the commanded motion is decided in the task space.

Assume $x_i, i = 1, \dots, n$ stands for the Cartesian position variables of the end effector. In order to connect the coordinates of the end effector with the joint coordinates, certain functions are used, $\theta_j, j = 1, \dots, m$, so the task space equation shall be

$$x_i = f_i(\theta_1, \dots, \theta_m) \quad i = 1, \dots, n \quad (2.19)$$

m is the number of the coordinates as presented in the joint space.

By differentiating Equation 3.1 once, this gives the following velocity relation.

$$\dot{x}_i = \sum_{j=1}^m \Gamma_{ij}^P \dot{\theta}_j \quad i = 1, \dots, n \quad (2.20)$$

And

$$\Gamma_{ij}^P = \frac{\partial f_i}{\partial \theta_j} \quad (2.21)$$

Equation (2.18) may be written in matrix for as

$$\dot{\hat{x}} = \hat{\Gamma}^P \dot{\hat{\theta}} \quad (2.22)$$

$\hat{\Gamma}^P$ is the $n \times m$ robot Jacobian matrix.

By making use of Equation 2.15, one can write the Jacobian matrix equation only in terms of the actuated variables. As a result the same series of steps is followed to find $n \times n$ matrix $\hat{\Gamma}^{Pa}$ and $n \times (m - n)$ matrix $\hat{\Gamma}^{Pu}$ as the corresponded joint variables coefficient matrices. This can be done as follows.

$$\hat{\Gamma}^{Pa} \dot{\bar{q}} + \hat{\Gamma}^{Pu} \dot{\bar{\theta}}^u = \dot{\bar{x}} \quad (2.23)$$

Substituting Equation 2.15 in into Equation 2.21 gives

$$\hat{\Gamma}^{Pa} \dot{\bar{q}} + \hat{\Gamma}^{Pu} \left[-(\hat{B}^u)^{-1} \hat{B}^a \dot{\bar{q}} \right] = \dot{\bar{x}} \quad (2.24)$$

Separating out the actuated variables joint coordinates vector gives

$$\dot{\bar{x}} = \hat{f} \dot{\bar{q}} \quad (2.25)$$

where \hat{f} is an $n \times n$ robot Jacobian matrix which is expressed as

$$\hat{f} = \hat{\Gamma}^{Pa} - \hat{\Gamma}^{Pu} \hat{B}^{u-1} \hat{B}^a \quad (2.26)$$

Equation 2.23 is differentiated up till snap level as follows.

$$\ddot{\bar{x}} = \dot{\hat{f}} \dot{\bar{q}} + \hat{f} \ddot{\bar{q}} \quad (2.27)$$

$$\ddot{\bar{x}} = \ddot{\hat{f}} \dot{\bar{q}} + 2\dot{\hat{f}} \ddot{\bar{q}} + \hat{f} \ddot{\bar{q}} \quad (2.28)$$

$$\ddot{\bar{x}} = \ddot{\hat{f}} \dot{\bar{q}} + 3\dot{\hat{f}} \ddot{\bar{q}} + \hat{f} \ddot{\bar{q}} \quad (2.29)$$

Hence,

$$\ddot{\bar{q}} = \hat{f}^{-1}(\ddot{x} - \ddot{\hat{f}}\bar{q} - 3\dot{\hat{f}}\dot{\bar{q}} - 3\hat{f}\ddot{\bar{q}}) \quad (2.30)$$

At this point, it's necessary to write the system equations of motion of the system by using only the actuated joint variables terms and this may be done by get rid of the non-actuated joint accelerations and the Lagrange multipliers λ that stand for the forces at the disconnected joints.

M and Q can be factorized into actuated and non-actuated joint variables as follows.

$$\hat{M} = \begin{bmatrix} \hat{M}^{aa} & \hat{M}^{au} \\ \hat{M}^{auT} & \hat{M}^{uu} \end{bmatrix} \quad (2.31)$$

and

$$\bar{Q} = \begin{bmatrix} \bar{Q}^a \\ \bar{Q}^u \end{bmatrix} \quad (2.32)$$

Where

\hat{M}^{aa} is an $n \times n$ sub-matrix that engendered by symmetric generalized mass matrix.

\hat{M}^{au} is an $n \times (m - n)$ sub-matrix that engendered by symmetric generalized mass matrix.

\hat{M}^{uu} is an $(m - n) \times (m - n)$ sub-matrix that engendered by symmetric generalized mass matrix.

\bar{Q}^a is an $n \times 1$ sub-matrix that engendered by \bar{Q} vector that includes Colriolis, centrifugal and gravitational terms.

\bar{Q}^u is an $(m - n) \times 1$ sub-matrix that engendered by Q vector that includes Colriolis, centrifugal and gravitational terms.

Equation 2.6 can be written now in two parts as follows.

$$\hat{M}^{aa}\ddot{q} + \hat{M}^{au}\ddot{\theta}^u + \bar{Q}^a + \hat{K}(\bar{q} - \bar{\phi}) - \hat{B}^{aT}\bar{\lambda} = 0 \quad (2.33a)$$

$$\hat{M}^{auT}\ddot{q} + \hat{M}^{uu}\ddot{\theta}^u + \bar{Q}^u - \hat{B}^{uT}\bar{\lambda} = 0 \quad (2.33b)$$

By eliminating $\bar{\lambda}$ after Substituting Equation 2.17 into Equation 2.32 and 2.33, the following n dimensional equations are obtained.

$$\hat{M}^*\ddot{q} + \bar{Q}^* + \hat{K}(\bar{q} - \bar{\phi}) = 0 \quad (2.34)$$

where,

$$\hat{M}^* = [\hat{M}^{aa} - \hat{M}^{au}\hat{B}^{u-1}\hat{B}^a] - \hat{B}^{aT}(\hat{B}^{u-1})^T [\hat{M}^{auT} - \hat{M}^{uu}\hat{B}^{u-1}\hat{B}^a] \quad (2.35)$$

$$\begin{aligned} \bar{Q}^* = & \left[-\hat{M}^{au}\hat{B}^{u-1}\dot{\hat{B}}^a + \hat{B}^{aT}(\hat{B}^{u-1})^T \hat{M}^{uu}\hat{B}^{u-1}\dot{\hat{B}}^a \right] \dot{q} \\ & + \left[-\hat{M}^{au}\hat{B}^{u-1}\dot{\hat{B}}^u + \hat{B}^{aT}(\hat{B}^{u-1})^T \hat{M}^{uu}\hat{B}^{u-1}\dot{\hat{B}}^u \right] \dot{\theta}^u \\ & + \bar{Q}^a - \hat{B}^{aT}(\hat{B}^{u-1})^T \bar{Q}^u \end{aligned} \quad (2.36)$$

After eliminating the intermediate variables \bar{q} and $\bar{\phi}$ in the dynamic equations, the following equation may show the relation between the input torques T and the output which is the independent end effector coordinates to accompany with constraint

surface x . After the elimination procedure as explained in [5], the input output relation is given as follows.

$$A(x)\ddot{x} + B(\ddot{x}, \dot{x}, x) = T \quad (2.37)$$

where,

$$A = \hat{K}^{-1} \hat{I}^r \hat{M} \hat{J}^{-1} \quad (2.38)$$

$$B = \hat{K}^{-1} \{ \hat{I}^r [-\hat{M}^* \hat{J}^{-1} (3\hat{J} \ddot{q} + \dot{\hat{J}} \dot{q} + \ddot{\hat{J}} \dot{q}) + 2\hat{M}^* \ddot{q} + \hat{M} \ddot{q} + \ddot{Q}^* + \hat{K} \ddot{q}] + \hat{M} \ddot{q} + \bar{Q}^* \} \quad (2.39)$$

By using the above equations, a feedback linearization (inverse dynamics) control method can be developed that will decouple and linearize the system. Numerical integration can be used for the purpose of calculating the corresponding control torque vector T yet, this course of action needs knowledge of \hat{M}^* , \ddot{M}^* , \dot{Q}^* , \ddot{Q}^* , \hat{J} and \ddot{J} and the resulting expressions will be too complex and long specifically for $n \geq 3$, which makes this method unsuitable for real time applications.

2.5.2 Control Law

The dynamic equations shall be used at the acceleration level so as to draw up an inverse feedback linearization (invers dynamics) control law for the purpose of finding the input torques needed to realize the desired end-effector motion.

Till this far, the system dynamic equations 2.34, 2.7, 2.27 may be presented in augmented form as follows.

$$\begin{bmatrix} \widehat{M}^* & 0 & 0 \\ 0 & \widehat{I}^r & -\widehat{I} \\ \widehat{J} & 0 & 0 \end{bmatrix} \begin{bmatrix} \ddot{\bar{q}} \\ \ddot{\bar{\phi}} \\ \ddot{\bar{T}} \end{bmatrix} = \begin{bmatrix} -\bar{Q}^* - \widehat{K}(\bar{q} - \bar{\phi}) \\ \widehat{K}(\bar{q} - \bar{\phi}) \\ -\widehat{J}\dot{\bar{q}} + \ddot{\bar{x}} \end{bmatrix} \quad (2.40)$$

Replacing $\ddot{\bar{x}}$ by the control variable z which stands for the command acceleration, it is seen from Equation 2.37 that in the forward dynamics problem, the torque vector \bar{T} instantly affects the end-effector jerk rate $\ddot{\bar{x}}$. As a result, the command jerk rates need to be decided in the control law. Utilizing the errors in the end-effector states and the desired jerk rates, the command jerk rates then can be formed as

$$\begin{aligned} \ddot{z} = & \bar{x}^{(4)d} + C_1(\bar{x}^{(3)d} - \bar{x}^{(3)}) + C_2(\ddot{\bar{x}}^d - \ddot{\bar{x}}) + C_3(\dot{\bar{x}}^d - \dot{\bar{x}}) \\ & + C_4(\bar{x}^d - \bar{x}) \end{aligned} \quad (2.41)$$

where the superscript d indicates desired values and C_1, C_2, C_3 and C_4 are constant feedback gain diagonal matrices, where $C_i = \text{diag}[C_{ij}], j = 1, \dots, n; i = 1, \dots, 4$.

As a matter of fact, at the inverse dynamics problem, only the first and the third rows of Equation 2.40 include the kinematic variables and may be short term as inverse kinematic equations. While, the second row of Equation 2.40 is utilized for the purpose of finding the control torques. Inertia and elastic force terms are included in the inverse kinematic equations as well due to redundancy caused by joint flexibility where inverse kinematic equations may be formed as follows.

$$\begin{bmatrix} \widehat{M}^* & 0 \\ \widehat{J} & 0 \end{bmatrix} \begin{bmatrix} \ddot{\bar{q}} \\ \ddot{\bar{\phi}} \end{bmatrix} = \begin{bmatrix} -\bar{Q}^* - \widehat{K}(\bar{q} - \bar{\phi}) \\ -\widehat{J}\dot{\bar{q}} + \bar{z} \end{bmatrix} \quad (2.42)$$

The above equation represents a singular package of differential equations so it can't be solved in that form. The reason behind singularity is that the ways of transmitting the control torques to the end-effector which is done through the elastic joints which make

the control torques do not have an instant effect on the acceleration of the end-effector. This causes the problem to be time-anticipatory. Equation 2.37 clearly showed that the torques do have an instant effect on the second derivative of the acceleration of the end-effector. In fact, an implicit numerical integration methods need to be used [5], because the acceleration coefficient matrix in Equation 2.42 is not able to be inverted to get an explicit system of ordinary differential equations. As an implicit numerical integration method, backward Euler method will be presented, the latter is one of the simplest implicit integration techniques where the integration is fully dependent of the following backward difference formula.

$$\dot{y}_{k+1} = \frac{1}{h}(y_{k+1} - y_k) \quad (2.43)$$

where h stands for the time interval and k represents the time step number. Using Eq. 2.43, Eq. 2.40 can be written at time t_{k+1} as

$$\hat{M}^* \frac{1}{h}(\dot{\bar{q}}_{k+1} - \dot{\bar{q}}_k) + \bar{Q}^* + \hat{K} (h\dot{\bar{q}}_{k+1} + \bar{q}_k - h\dot{\bar{\phi}}_{k+1} - \bar{\phi}_k) = 0 \quad (2.44)$$

$$\hat{I}r \frac{1}{h}(\dot{\bar{\phi}}_{k+1} - \dot{\bar{\phi}}_k) - \hat{K} (h\dot{\bar{q}}_{k+1} + \bar{q}_k - h\dot{\bar{\phi}}_{k+1} - \bar{\phi}_k) = \bar{T}_{k+1} \quad (2.45)$$

$$\hat{J} \frac{1}{h}(\dot{\bar{q}}_{k+1} - \dot{\bar{q}}_k) + \hat{J}\dot{\bar{q}}_{k+1} = z_{k+1} \quad (2.46)$$

where $\hat{M}^*(h\dot{\bar{q}}_{k+1} + \bar{q}_k)$, $\bar{Q}^*(h\dot{\bar{q}}_{k+1} + \bar{q}_k, \dot{\bar{q}}_{k+1})$, $J(h\dot{\bar{q}}_{k+1} + \bar{q}_k)$ and $\hat{J}(h\dot{\bar{q}}_{k+1} + \bar{q}_k, \dot{\bar{q}}_{k+1})$ also depend on $\dot{\bar{q}}_{k+1}$. Equations (2.44-2.46) are a set of $3n$ algebraic equations that solved for the $3n$ unknowns $\dot{\bar{q}}_{k+1}$, $\dot{\bar{\phi}}_{k+1}$ and \bar{T}_{k+1} as below. The term z appears in Equation 2.46 shall be obtained by integration of Equation 2.41. Piecewise smooth functions for is utilized to decide the desired motion.

In the time interval $t_a < t < t_b$, assume $x^d(t)$ be smooth till the third derivative. Then by integration of Equation 2.41 twice at this time interval gives.

$$\begin{aligned}
z - z_a - \dot{z}_a(t - t_a) &= \ddot{x}^d - \ddot{x}_a^d - \ddot{x}_a^d(t - t_a) + C_1[(\dot{x}^d - \dot{x}) - (\dot{x}_a^d - \dot{x}_a) - \\
&(\ddot{x}_a^d - \ddot{x}_a)(t - t_a)] + C_2[(x^d - x) - (x_a^d - x_a) - (\dot{x}_a^d - \dot{x}_a)(t - t_a)] - C_3(x_a^d - \\
&x_a)(t - t_a) + C_3 \int_{t_a}^t \ddot{w}(\tau) d\tau + C_4 \int_{t_a}^t [\int_{t_a}^{\tau} \ddot{w}(s) ds] d\tau, \tag{2.47}
\end{aligned}$$

$$t_a < t < t_b$$

where $\ddot{w} = x^d - x$.

Evaluation of Equation (2.47) at time t_{k+1} gives

$$\begin{aligned}
\bar{z}_{k+1} &= \bar{z}_a + \dot{\bar{z}}_a(t_{k+1} - t_a) + \ddot{\bar{x}}_{k+1}^d - \ddot{\bar{x}}_a^d - \ddot{\bar{x}}_a^d(t_{k+1} - t_a) + \hat{C}_1[(\dot{\bar{x}}_{k+1}^d - \dot{\bar{x}}_{k+1} - \\
&(\dot{\bar{x}}_a^d - \dot{\bar{x}}_a) - (\ddot{\bar{x}}_a^d - \ddot{\bar{x}}_a)(t_{k+1} - t_a)] + \hat{C}_2[(\bar{x}_{k+1}^d - \bar{x}_{k+1}) - (\bar{x}_a^d - \bar{x}_a) - (\dot{\bar{x}}_a^d - \\
&\dot{\bar{x}}_a)(t_{k+1} - t_a)] - \hat{C}_3(\bar{x}_a^d - \bar{x}_a)(t_{k+1} - t_a) + \hat{C}_3(h\ddot{\bar{w}}_{k+1} + \dot{\bar{w}}_k) + \hat{C}_4(h^2\ddot{\bar{w}}_{k+1} + h\dot{\bar{w}}_k + \\
&\bar{w}_k), \tag{2.48}
\end{aligned}$$

$$t_a \leq t_{k+1} \leq t_b$$

where $\ddot{\bar{w}}_{k+1} = \bar{x}_{k+1}^d - \bar{x}_{k+1}$.

Moreover, to stay away from any jump of the command accelerations z and their derivatives \dot{z} caused by that the control torques does not hold an instant effect on the end-effector jerks and acceleration and this can be done by decide the integration constants to be the same as z and \dot{z} at the intermissions of the desired motion. This is obtained by selecting the integration constants such a way that:

$\bar{z}_a = \bar{z}(t_a^+) = \bar{z}(t_a^-)$ and $\dot{\bar{z}}_a = \dot{\bar{z}}(t_a^+) = \dot{\bar{z}}(t_a^-)$. (When the system start from the rest, then $\bar{z}_0 = 0, \dot{\bar{z}}_0 = 0$).

In any singular package of differential equations, the initial conditions are not autonomous according to [4]. The initial conditions must satisfy specified relations found by using Equation 2.42. Premultiplying the second row of the latter Equation and subtracting the result from the first row, gives

$$\widehat{M}^* \widehat{f}^{-1} \left(-\dot{\widehat{f}} \bar{q} + \bar{z} \right) + \bar{Q}^* + \widehat{K}(\bar{q} - \bar{\phi}) = 0 \quad (2.49)$$

To find the control torque \bar{T}_{k+1} by using Equations (2.44-2.46), the initial values of q_k, ϕ_k and \dot{q}_k are required. When $\bar{q}_k, \bar{\phi}_k$ and $\dot{\bar{q}}_k$ are calculated at time t_k , they will not satisfy Equation (2.49) when disturbance and modeling error are existed. This conflict results the control torques to be incorrect. As a matter of fact, when $h \rightarrow 0$, they diverge. To attain the consistency, one may solve Equation (2.49) for $\bar{\phi}_k$ or $\dot{\bar{\phi}}_k$. Choosing $\bar{\phi}_k$ for this aim it can be gained by using Equation (2.49) at time t_k as

$$\bar{\phi}_k = \bar{q}_k + \widehat{K}^{-1} \left\{ \widehat{M}^* \widehat{f}^{-1} \left(-\dot{\widehat{f}} \bar{q}_k + \bar{z}_k \right) + \bar{Q}^* \right\} \quad (2.50)$$

where \bar{q}_k and $\dot{\bar{q}}_k$ are the measured quantities.

Equation (2.46) stands for n nonlinear algebraic equations solved for $\dot{\bar{q}}_{k+1}$. \bar{z}_{k+1} in Equation (2.46) is given by Equation (2.48) where \bar{x}_k and $\dot{\bar{x}}_k$ are calculated from \bar{q}_k and $\dot{\bar{q}}_k$ by using Equation (2.25) and its' integration. Then Equation (2.44) is put to use to find $\dot{\bar{\phi}}_{k+1}$ as

$$\dot{\bar{\phi}}_{k+1} = (\widehat{K}h)^{-1} \left[\widehat{M}^* \frac{1}{h} (\dot{\bar{q}}_{k+1} - \dot{\bar{q}}_k) + \bar{Q}^* + \widehat{K}(\bar{q}_k - \bar{\phi}_k) \right] + \dot{\bar{q}}_{k+1} \quad (2.51)$$

Finally, the control torques \bar{T}_{k+1} are calculated from Equation 2.45.

2.5.3 Position Error Dynamics

The computed torques by (2.40) Equation linearize and decouple the command jerks. To show that, consider that, the actual accelerations are similar to the command accelerations i.e. $\ddot{x} = z$ in the obscurity of error in modeling and this gives the following error dynamics.

$$\bar{e}^{(4)} + \hat{C}_1 \bar{e}^{(3)} + \hat{C}_2 \ddot{\bar{e}} + \hat{C}_3 \dot{\bar{e}} + \hat{C}_4 \bar{e} = 0 \quad (2.52)$$

where $\bar{e} = \bar{x}^d - \bar{x}$. Asymptotic stability is reached by suitable selection of feedback gains. To do this, performance indices such as Integral Square Error (ISE), Integral of the Absolute Magnitude of Error (IAE), Integral Time Absolute Error (ITAE) and Integral Time Square Error (ITSE) can be used. In this study ITAE performance index which is shown below will be used.

$$ITAE = \int_0^T t|e(t)|dt \quad (2.53)$$

Effect of large initial errors is reduced while small errors in long-term are vanished, this happens by using ITAE performance index and because of the multiplication by time t.

For closed-loop system, the form of property equation that based on ITAE standard is $s^n + C_1 s^{n-1} + C_2 s^{n-2} + \dots + C_n$. To satisfy the ITAE criteria, the feedback diagonal matrices $C_j, j = 1,2,3,4$ are chosen as such that

$C_{1i} = 2.1\omega_i, C_{2i} = 3.4\omega_i^2, C_{3i} = 2.7\omega_i^3, C_4 = \omega_i^4, i = 1,2,3$; where ω_i is a positive constant.

CHAPTER 3

THREE REVOLUTE JOINTS THREE LEGS PLANAR PARALLEL ROBOT STUDY AND SIMULATION

3.1 Planar Parallel Robot Study

To explain and test the execution of the control law presented in the previous chapter, a planar parallel robot shown in Figure 3.1 and Figure 3.2 is regarded. Parallel robots are usually defined according to the number of legs from the base to the platform as well as the type and number of the joints these legs have. The 3-RRR parallel robot shown below is to be studied, where 3-RRR means that the robot has three legs each one of them has three revolute joints between the fixed base and the moving platform.

The robot is supported with a fixed surface which is in contact with the end-effector and this surface is a fixed plane parallel to the x - z plane. This study focuses completely on the motion control where the contact forces and force control are not considered.

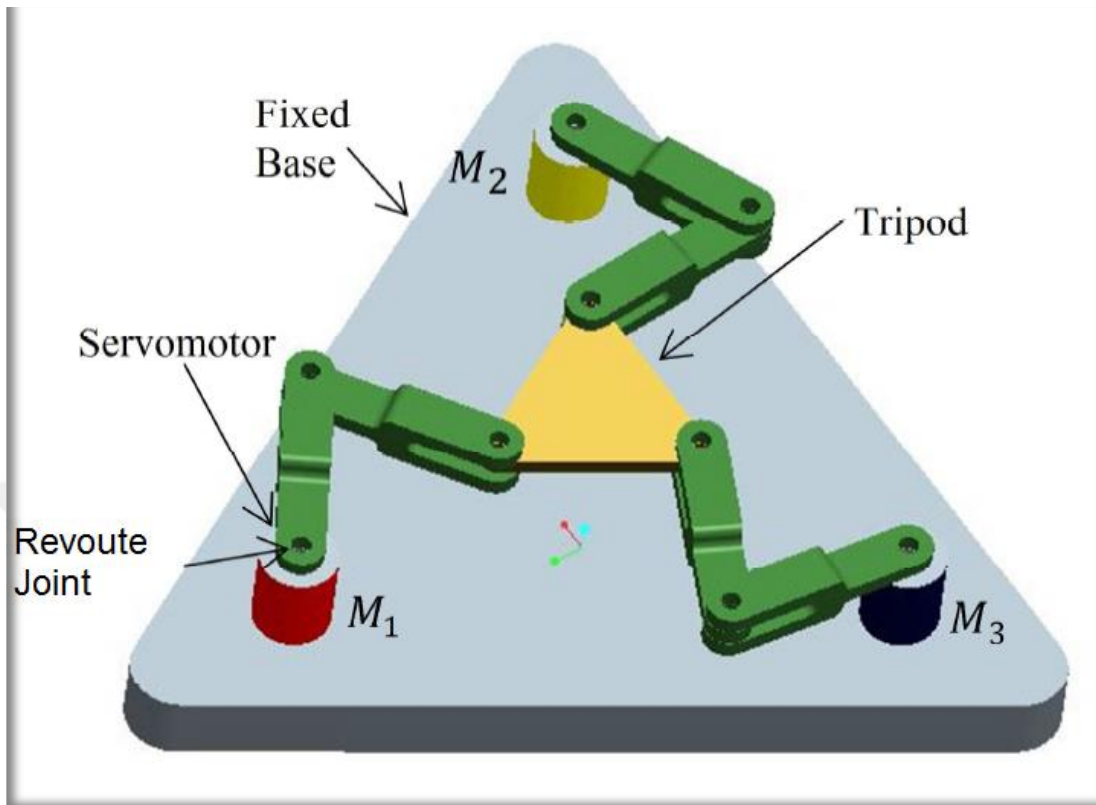


Figure 2 3-RRR Planar Parallel Robot Architecture

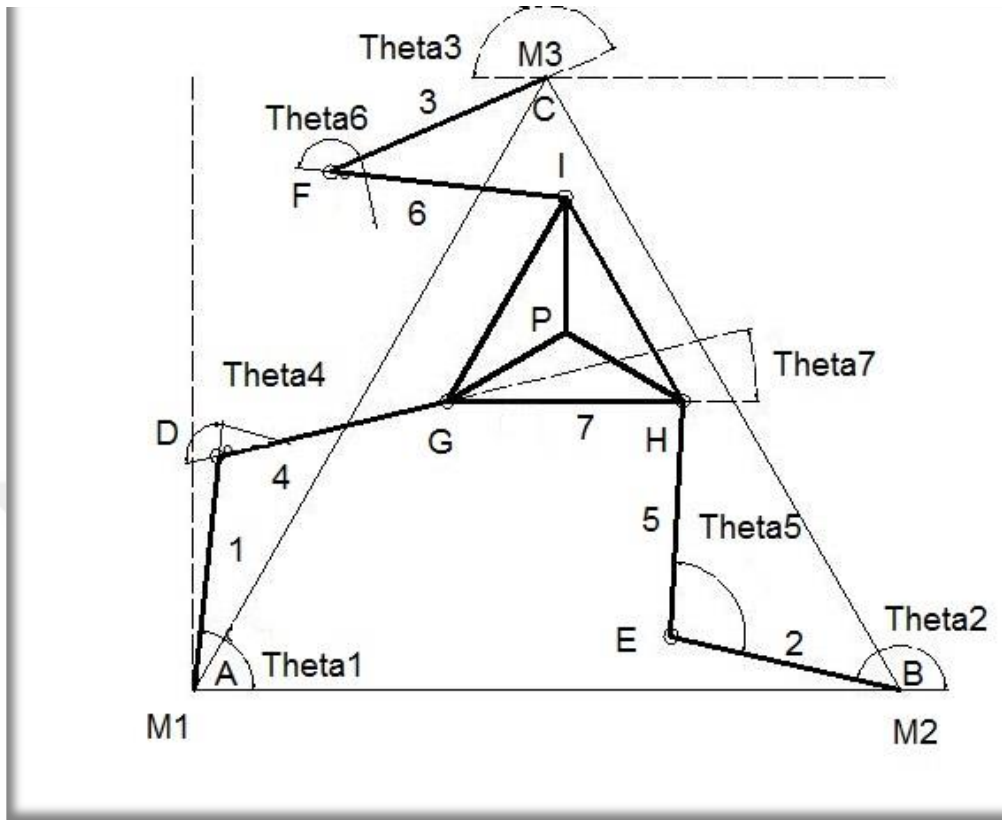


Figure 3 3-RRR Planar Parallel Robot

Where, M1, M2, M3 are the three actuating motors.

The system has eight links regarding the fixed link and nine revolute joints. Actuators that located on A, B and C are actuating the system by the generated torques and θ_1, θ_2 and θ_3 are the joint variables of A, B and C respectively. The robot has a total of six degrees of freedom because of the three added degrees of freedom of the flexible joints. The motors rotation is perpendicular to the plane of the motion and the weight's action is in the $-y$ direction.

Vectors of joint variables and actuator variables has been defined already in chapter 2, the vector of the joints variables may be split into actuated and non-actuated sub-vectors as below.

$$\bar{\theta} = [\bar{q}^T \ \bar{\theta}^{uT}]^T \quad (3.1)$$

3.1.1 Kinetic Energy

Expressions of the kinetic energy can be got by substituting the components of the translational and angular velocities of each link and actuator in the following equations of kinetic energy of any link and actuator.

Kinetic energy of the i^{th} link:

$$KE_{Li} = \frac{1}{2} m_i^L (\bar{V}_{Gi}^L)^T \bar{V}_{Gi}^L + \frac{1}{2} (\bar{\omega}_i^L)^T \hat{I}_i^L \bar{\omega}_i^L \quad (3.5)$$

Where,

$$\bar{V}_{Gi}^L = \sum_{j=1}^m \bar{W}_{ij}^L \dot{\theta}_j \quad (3.6)$$

$$\bar{\omega}_i^L = \sum_{j=1}^m \bar{\Omega}_{ij}^L \dot{\theta}_j \quad (3.7)$$

$$\hat{I}_i^L = [\hat{C}^{(0,i)}] \hat{I}_{-i}^L [\hat{C}^{(0,i)}]^T \quad (3.8)$$

In the equations above,

m_i^L is the i^{th} link's mass, \bar{V}_{Gi}^L is the vector of the i^{th} link's mass center velocity that presented in the fixed reference frame, \bar{W}_{ij}^L is the coefficient vector of the velocity influence, $\bar{\omega}_i^L$ is the i^{th} link's angular velocity that presented in the fixed reference frame, $\bar{\Omega}_{ij}^L$ is the angular coefficient vector of the velocity influence, \hat{I}_i^L is the i^{th} link's moment of inertia matrix presented in the fixed reference frame, $\hat{C}^{(0,i)}$ is the transformation matrix from the reference frame of the i^{th} link to the fixed reference frame and \hat{I}_{-i}^L is the i^{th} link's moment of inertia matrix presented in its body reference frame.

Kinetic energy of the i^{th} actuator:

$$KE_{Ai} = \frac{1}{2} m_i^A (\bar{V}_{Gi}^A)^T \bar{V}_{Gi}^A + \frac{1}{2} I_i^A \dot{t}_i^2 \quad (3.8)$$

Link-1

$$\bar{r}_{G_1}^{(0)} = \frac{L_1}{2}(c\theta_1 + s\theta_1) \quad (3.9)$$

$$\bar{V}_{G_1}^{(0)} = \dot{\bar{r}}_{G_1}^{(0)} = \frac{L_1}{2}(-s\theta_1\dot{\theta}_1 + c\theta_1\dot{\theta}_1) = \begin{bmatrix} -\frac{L_1}{2}s\theta_1\dot{\theta}_1 \\ \frac{L_1}{2}c\theta_1\dot{\theta}_1 \\ 0 \end{bmatrix} \quad (3.10)$$

$$\bar{\omega}_1^{(0)} = \begin{bmatrix} 0 \\ 0 \\ \dot{\theta}_1 \end{bmatrix} \quad (3.11)$$

As a result, kinetic energy related to Link-1 is presented as

$$KE_{L1} = \frac{1}{2} \left[m_1^L \frac{L_1^2}{4} + I_{1zz} \right] \quad (3.12)$$

Link-2

$$\bar{r}_{G_2}^{(0)} = \frac{L_2}{2}(c\theta_2 + s\theta_2) \quad (3.13)$$

$$\bar{V}_{G_2}^{(0)} = \dot{\bar{r}}_{G_2}^{(0)} = \frac{L_2}{2}(-s\theta_2\dot{\theta}_2 + c\theta_2\dot{\theta}_2) = \begin{bmatrix} -\frac{L_2}{2}s\theta_2\dot{\theta}_2 \\ \frac{L_2}{2}c\theta_2\dot{\theta}_2 \\ 0 \end{bmatrix} \quad (3.14)$$

$$\bar{\omega}_2^{(0)} = \begin{bmatrix} 0 \\ 0 \\ \dot{\theta}_2 \end{bmatrix} \quad (3.15)$$

As a result, kinetic energy related to Link-2 is presented as

$$KE_{L2} = \frac{1}{2} \left[m_2^L \frac{L_2^2}{4} + I_{2zz} \right] \quad (3.16)$$

Link-3

$$\bar{r}_{G_3}^{(0)} = \frac{L_3}{2}(c\theta_3 + s\theta_3) \quad (3.17)$$

$$\bar{V}_{G_3}^{(0)} = \dot{\bar{r}}_{G_3}^{(0)} = \frac{L_3}{2}(-s\theta_3\dot{\theta}_3 + c\theta_3\dot{\theta}_3) = \begin{bmatrix} -\frac{L_3}{2}s\theta_3\dot{\theta}_3 \\ \frac{L_3}{2}c\theta_3\dot{\theta}_3 \\ 0 \end{bmatrix} \quad (3.18)$$

$$\bar{\omega}_3^{(0)} = \begin{bmatrix} 0 \\ 0 \\ \dot{\theta}_3 \end{bmatrix} \quad (3.19)$$

As a result, kinetic energy related to Link-3 is presented as

$$KE_{L3} = \frac{1}{2} \left[m_3 \frac{L_3^2}{4} + I_{3zz} \right] \quad (3.20)$$

Link-4

$$\bar{r}_{G_4}^{(0)} = L_1(c\theta_1 + s\theta_1) + \frac{L_4}{2}(c\theta_{14} + s\theta_{14}) \quad (3.21)$$

$$\begin{aligned} \bar{V}_{G_4}^{(0)} &= L_1(-s\theta_1\dot{\theta}_1 + c\theta_1\dot{\theta}_1) + \frac{L_4}{2}(-s\theta_{14}\dot{\theta}_{14} + c\theta_{14}\dot{\theta}_{14}) \\ &= \begin{bmatrix} -L_1s\theta_1\dot{\theta}_1 - \frac{L_4}{2}s\theta_{14}\dot{\theta}_{14} \\ L_1c\theta_1\dot{\theta}_1 + \frac{L_4}{2}c\theta_{14}\dot{\theta}_{14} \\ 0 \end{bmatrix} \end{aligned} \quad (3.22)$$

$$\bar{\omega}_4^{(0)} = \begin{bmatrix} 0 \\ 0 \\ \dot{\theta}_{14} \end{bmatrix} \quad (3.23)$$

As a result, kinetic energy related to Link-4 is presented as

$$KE_{L4} = \frac{1}{2} m_4 L_1^2 \dot{\theta}_1^2 + \frac{1}{2} m_4 L_1 L_4 c(\theta_1 - \theta_{14}) \dot{\theta}_1 (\dot{\theta}_1 + \dot{\theta}_4)$$

$$+1/2 \left[m_4^L \frac{L_4^L}{4} + I_{4zz} \right] (\dot{\theta}_1 + \dot{\theta}_4)^2 \quad (3.24)$$

Link-5

$$\bar{r}_{G_5}^{(0)} = L_2(c\theta_2 + s\theta_2) + \frac{L_5}{2}(c\theta_{25} + s\theta_{25}) \quad (3.25)$$

$$\bar{V}_{G_5}^{(0)} = L_2(-s\theta_2\dot{\theta}_2 + c\theta_2\dot{\theta}_2) + \frac{L_5}{2}(-s\theta_{25}\dot{\theta}_{25} + c\theta_{25}\dot{\theta}_{25})$$

$$= \begin{bmatrix} -L_2s\theta_2\dot{\theta}_2 - \frac{L_5}{2}s\theta_{25}\dot{\theta}_{25} \\ L_2c\theta_2\dot{\theta}_2 + \frac{L_4}{2}c\theta_{25}\dot{\theta}_{25} \\ 0 \end{bmatrix} \quad (3.26)$$

$$\bar{\omega}_5^{(0)} = \begin{bmatrix} 0 \\ 0 \\ \dot{\theta}_{25} \end{bmatrix} \quad (3.27)$$

As a result, kinetic energy related to Link-5 is presented as

$$KE_{L5} = \frac{1}{2}m_5^L L_2^2 \dot{\theta}_2^2 + \frac{1}{2}m_5^L L_2 L_5 c(\theta_2 - \theta_{25}) \dot{\theta}_2 (\dot{\theta}_2 + \dot{\theta}_{25}) + \frac{1}{2} \left[m_5^L \frac{L_5^L}{4} + I_{5zz} \right] (\dot{\theta}_2 + \dot{\theta}_5)^2 \quad (3.28)$$

Link-6

$$\bar{r}_{G_6}^{(0)} = L_3(c\theta_3 + s\theta_3) + \frac{L_5}{2}(c\theta_{36} + s\theta_{36}) \quad (3.29)$$

$$\bar{V}_{G_6}^{(0)} = L_3(-s\theta_3\dot{\theta}_3 + c\theta_3\dot{\theta}_3) + \frac{L_5}{2}(-s\theta_{36}\dot{\theta}_{36} + c\theta_{36}\dot{\theta}_{36})$$

$$= \begin{bmatrix} -L_3s\theta_3\dot{\theta}_3 - \frac{L_6}{2}s\theta_{36}\dot{\theta}_{36} \\ L_3c\theta_3\dot{\theta}_3 + \frac{L_4}{2}c\theta_{36}\dot{\theta}_{36} \\ 0 \end{bmatrix} \quad (3.30)$$

$$\bar{\omega}_5^{(0)} = \begin{bmatrix} 0 \\ 0 \\ \dot{\theta}_{25} \end{bmatrix} \quad (3.31)$$

As a result, kinetic energy related to Link-6 is presented as

$$\begin{aligned} KE_{L5} &= \frac{1}{2} m_6^L L_3^2 \dot{\theta}_3^2 + \frac{1}{2} m_6^L L_3 L_6 c(\theta_3 - \theta_{36}) \dot{\theta}_3 (\dot{\theta}_3 + \dot{\theta}_{36}) \\ &\quad + \frac{1}{2} \left[m_6^L \frac{L_6^2}{4} + I_{6zz} \right] (\dot{\theta}_3 + \dot{\theta}_6)^2 \end{aligned} \quad (3.32)$$

Link-7

$$\begin{aligned} \bar{r}_{G7}^{(0)} &= L_1(c\theta_1 + s\theta_1) + L_4(c\theta_{14} + s\theta_{14}) \\ &\quad + d_7[c(\theta_{147} + \beta) + s(\theta_{147} + \beta)] \end{aligned} \quad (3.33)$$

$$\bar{V}_{G7}^{(0)} = \begin{bmatrix} -L_1 s\theta_1 \dot{\theta}_1 - L_4 s\theta_{14} \dot{\theta}_{14} - d_7 s(\theta_{147} + \beta) \dot{\theta}_{147} \\ L_1 c\theta_1 \dot{\theta}_1 + L_4 c\theta_{14} \dot{\theta}_{14} + d_7 c(\theta_{147} + \beta) \dot{\theta}_{147} \\ 0 \end{bmatrix} \quad (3.34)$$

$$\bar{\omega}_7^{(0)} = \begin{bmatrix} 0 \\ 0 \\ \dot{\theta}_{147} \end{bmatrix} \quad (3.35)$$

As a result, kinetic energy related to Link-7 is presented as

$$\begin{aligned} KE_{L7} &= \frac{1}{2} m_7^L L_1^2 \dot{\theta}_1 + \frac{1}{2} m_7^L L_4^2 (\dot{\theta}_1 + \dot{\theta}_4)^2 + \frac{1}{2} [m_7^L g_7^2 + I_{7zz}] (\dot{\theta}_1 + \dot{\theta}_4 + \dot{\theta}_7)^2 \\ &\quad + m_7^L L_1 L_4 c(\theta_1 - \theta_{14}) \dot{\theta}_1 (\dot{\theta}_1 + \dot{\theta}_4) \\ &\quad + m_7^L L_1 g_7 c(\theta_1 - \theta_{147} - \beta) \dot{\theta}_1 (\dot{\theta}_1 + \dot{\theta}_4 + \dot{\theta}_7) \\ &\quad + m_7^L L_4 g_7 (\theta_{14} - \theta_{147} - \beta) (\dot{\theta}_1 + \dot{\theta}_4) \end{aligned} \quad (3.36)$$

Actuator-1

$$\bar{V}_1^A = \bar{0} \quad (3.37)$$

$$\bar{\omega}_1^A = \begin{bmatrix} 0 \\ 0 \\ r_1 \dot{\phi}_1 \end{bmatrix} \quad (3.38)$$

As a result, kinetic energy related to Actuator-1 is presented as

$$KE_{A1} = \frac{1}{2} [r_1^2 I_{1zz}^r] \dot{\phi}_1^2 \quad (3.39)$$

Actuator-2

$$\bar{V}_2^A = \bar{0} \quad (3.40)$$

$$\bar{\omega}_2^A = \begin{bmatrix} 0 \\ 0 \\ r_2 \dot{\phi}_2 \end{bmatrix} \quad (3.41)$$

As a result, kinetic energy related to Actuator-2 is presented as

$$KE_{A2} = \frac{1}{2} [r_2^2 I_{2zz}^r] \dot{\phi}_2^2 \quad (3.42)$$

Actuator-3

$$\bar{V}_3^A = \bar{0} \quad (3.43)$$

$$\bar{\omega}_3^A = \begin{bmatrix} 0 \\ 0 \\ r_3 \dot{\phi}_3 \end{bmatrix} \quad (3.44)$$

As a result, kinetic energy related to Actuator-1 is presented as

$$KE_{A3} = \frac{1}{2} [r_3^2 I_{3zz}^r] \dot{\phi}_3^2 \quad (3.45)$$

The sum of links and actuators kinetic energy values represents the total kinetic energy of the system.

The Lagrange components related to the kinetic energy are given as follow.

$$\begin{aligned}
\frac{d}{dt} \left(\frac{\partial K}{\partial \dot{\theta}_1} \right) &= \ddot{\theta}_1 \left\{ \left(m_1^L \frac{L_1^2}{4} + I_{1zz} \right) + m_4^L L_1^2 + m_4^L L_1 L_4 c(-\theta_4) + \left[m_4^L \frac{L_4^2}{4} + I_{4zz} \right] + m_7^L L_1^2 + \right. \\
& m_7^L L_4^2 + [m_7^L g_7^2 + I_{7zz}] + 2m_7^L L_1 L_4 c(-\theta_4) + 2m_7^L L_1 g_7 c[-(\theta_4 + \theta_7 + \beta)] + \\
& \left. 2m_7^L L_4 g_7 c[-(\theta_7 + \beta)] \right\} + \ddot{\theta}_4 \left\{ m_4^L \frac{L_1}{2} L_4 c(-\theta_4) + \left[m_4^L \frac{L_4^2}{4} + I_{4zz} \right] + m_7^L L_4^2 + \right. \\
& [m_7^L g_7^2 + I_{7zz}] + m_7^L L_1 L_4 c(-\theta_4) + m_7^L L_1 g_7 c[-(\theta_4 + \theta_7 + \beta)] + 2m_7^L L_4 g_7 c[-(\theta_7 + \\
& \left. \beta)] \right\} + \ddot{\theta}_7 \{ (m_7^L g_7^2 + I_{7zz}) + M_7^L L_1 g_7 c[-(\theta_4 + \theta_7 + \beta)] + M_7^L L_4 g_7 c[-(\theta_7 + \\
& \left. \beta)] \} \tag{3.46}
\end{aligned}$$

$$\begin{aligned}
\frac{d}{dt} \left(\frac{\partial K}{\partial \dot{\theta}_2} \right) &= \ddot{\theta}_2 \left\{ \left[m_2^L \frac{L_2^2}{4} + I_{2zz} \right] + m_5^L L_2^2 + M_5^L L_2 L_5 c(-\theta_5) + \left[m_5^L \frac{L_5^2}{4} + I_{5zz} \right] \right\} \\
& + \ddot{\theta}_5 \left\{ \frac{1}{2} m_5^L L_2 L_5 c(-\theta_5) + \left[m_5^L \frac{L_5^2}{4} + I_{5zz} \right] \right\} \tag{3.47}
\end{aligned}$$

$$\begin{aligned}
\frac{d}{dt} \left(\frac{\partial K}{\partial \dot{\theta}_3} \right) &= \ddot{\theta}_3 \left\{ \left[m_3^L \frac{L_3^2}{4} + I_{3zz} \right] + m_6^L L_3^2 + M_6^L L_3 L_6 c(-\theta_6) + \left[m_6^L \frac{L_6^2}{4} + I_{6zz} \right] \right\} \\
& + \ddot{\theta}_6 \left\{ \frac{1}{2} m_6^L L_3 L_6 c(-\theta_6) + \left[m_6^L \frac{L_6^2}{4} + I_{6zz} \right] \right\} \tag{3.48}
\end{aligned}$$

$$\begin{aligned}
\frac{d}{dt} \left(\frac{\partial K}{\partial \dot{\theta}_4} \right) &= \ddot{\theta}_4 \left\{ \left[m_4^L \frac{L_4^2}{4} + I_{4zz} \right] + m_7^L L_4^2 + [m_7^L g_7^2 + I_{7zz}] + 2m_7^L c[-(\theta_7 + \beta)] \right\} \\
& + \ddot{\theta}_1 \left\{ \left(\frac{1}{2} m_4^L L_1 L_4 c(-\theta_4) + \left[m_4^L \frac{L_4^2}{4} + I_{4zz} \right] + m_7^L L_4^2 + [m_7^L g_7^2 + I_{7zz}] + \right. \right. \\
& \left. \left. m_7^L L_1 L_4 c(-\theta_4) + m_7^L L_1 g_7 c[-(\theta_4 + \theta_7 + \beta)] + 2m_7^L L_4 g_7 c[-(\theta_7 + \beta)] \right\} \right. \\
& \left. + \ddot{\theta}_7 \{ [m_7^L g_7^2 + I_{7zz}] + m_7^L L_4 g_7 c[-(\theta_7 + \beta)] \} \tag{3.49}
\end{aligned}$$

$$\frac{d}{dt} \left(\frac{\partial K}{\partial \dot{\theta}_5} \right) = \ddot{\theta}_5 \left\{ \left[m_5^L \frac{L_5^2}{4} + I_{5zzz} \right] \right\} + \ddot{\theta}_2 \left\{ \frac{1}{2} L_2 L_5 c(-\theta_5) + \left[m_5^L \frac{L_5^2}{4} + I_{5zzz} \right] \right\} \quad (3.50)$$

$$\frac{d}{dt} \left(\frac{\partial K}{\partial \dot{\theta}_6} \right) = \ddot{\theta}_6 \left\{ \left[m_6^L \frac{L_6^2}{4} + I_{6zzz} \right] \right\} + \ddot{\theta}_3 \left\{ \frac{1}{2} 3L_6 c(-\theta_6) + \left[m_6^L \frac{L_6^2}{4} + I_{6zzz} \right] \right\} \quad (3.51)$$

$$\begin{aligned} \frac{d}{dt} \left(\frac{\partial K}{\partial \dot{\theta}_7} \right) &= \ddot{\theta}_7 \{ [m_7^L g_7^2 + I_{7zz}] \} + \ddot{\theta}_1 \{ [m_7^L g_7^2 + I_{7zz}] + m_{7L} L_1 g_7 c[-(\theta_4 + \theta_7 + \beta)] + \\ & m_7^L g_7 c[-(\theta_7 + \beta)] \} + \ddot{\theta}_4 \{ [m_7^L g_7^2 + I_{7zz}] + m_7^L g_7 c[-(\theta_7 + \beta)] \} \end{aligned} \quad (3.52)$$

$$\frac{d}{dt} \left(\frac{\partial K}{\partial \dot{\phi}_1} \right) = \ddot{\phi}_1 [r_1^2 I_{1zz}^r] \quad (3.53)$$

$$\frac{d}{dt} \left(\frac{\partial K}{\partial \dot{\phi}_2} \right) = \ddot{\phi}_2 [r_2^2 I_{2zz}^r] \quad (3.54)$$

$$\frac{d}{dt} \left(\frac{\partial K}{\partial \dot{\phi}_3} \right) = \ddot{\phi}_3 [r_3^2 I_{3zz}^r] \quad (3.55)$$

$$\frac{\partial K}{\partial \theta_1} = 0 \quad (3.56)$$

$$\frac{\partial K}{\partial \theta_2} = 0 \quad (3.57)$$

$$\frac{\partial K}{\partial \theta_3} = 0 \quad (3.58)$$

$$\begin{aligned} \frac{\partial K}{\partial \theta_4} &= \frac{1}{2} \dot{\theta}_1^2 \{ m_4^L L_1 L_4 s(-\theta_4) + 2m_7^L L_1 L_4 s(-\theta_4) + 2m_7^L L_1 d_7 s[-(\theta_4 + \theta_7 + \beta)] \} + \\ & \dot{\theta}_1 \dot{\theta}_4 \left\{ \frac{1}{2} m_4^L L_1 L_4 s(-\theta_4) + m_7^L L_1 L_4 s(-\theta_4) + m_7^L L_1 d_7 s[-(\theta_4 + \theta_7 + \beta)] \right\} + \\ & \dot{\theta}_1 \dot{\theta}_7 \{ m_7^L L_1 d_7 s[-(\theta_4 + \theta_7 + \beta)] \} \end{aligned} \quad (3.59)$$

$$\frac{\partial K}{\partial \theta_5} = \frac{1}{2} \dot{\theta}_2^2 m_5^L L_2 L_5 s(-\theta_5) + \dot{\theta}_2 \dot{\theta}_5 \frac{1}{2} m_5^L L_2 L_5 s(-\theta_5) \quad (3.60)$$

$$\frac{\partial K}{\partial \theta_6} = \frac{1}{2} \dot{\theta}_3^2 m_6^L L_3 L_6 s(-\theta_6) + \dot{\theta}_3 \dot{\theta}_6 \frac{1}{2} m_6^L L_3 L_6 s(-\theta_6) \quad (3.61)$$

$$\begin{aligned} \frac{\partial K}{\partial \theta_7} = & \dot{\theta}_1^2 \{m_7^L L_1 d_7 s[-(\theta_4 + \theta_7 + \beta)] + m_7^L L_4 d_7 s[-(\theta_7 + \beta)]\} + \dot{\theta}_4^2 \{m_7^L L_4 d_7 s[-(\theta_7 + \\ & \beta)]\} + \dot{\theta}_1 \dot{\theta}_4 [m_7^L L_1 d_7 s[-(\theta_4 + \theta_7 + \beta)] + 2m_7^L L_4 d_7 s[-(\theta_7 + \beta)]] + \\ & \dot{\theta}_1 \dot{\theta}_7 \{m_7^L L_1 d_7 s[-(\theta_4 + \theta_7 + \beta)] + m_7^L d_7 s[-(\theta_7 + \beta)]\} + \dot{\theta}_4 \dot{\theta}_7 \{m_7^L L_4 d_7 s[-(\theta_7 + \\ & \beta)]\} \end{aligned} \quad (3.62)$$

$$\frac{\partial K}{\partial \phi_1} = 0 \quad (3.63)$$

$$\frac{\partial K}{\partial \phi_2} = 0 \quad (3.64)$$

$$\frac{\partial K}{\partial \phi_3} = 0 \quad (3.65)$$

3.1.2 Potential Energy

Potential energy formulas of links and actuators are given as follow.

$$PE_{L1} = m_1^L g \frac{L_1}{2} s\theta_1 \quad (3.66)$$

$$PE_{L2} = m_2^L g \frac{L_2}{2} s\theta_2 \quad (3.67)$$

$$PE_{L3} = m_3^L g \frac{L_3}{2} s\theta_3 \quad (3.68)$$

$$PE_{L4} = m_4^L g \left[L_1 s\theta_1 + \frac{L_4}{2} s(\theta_{14}) \right] \quad (3.69)$$

$$PE_{L5} = m_5^L g \left[L_2 s\theta_2 + \frac{L_5}{2} s(\theta_{25}) \right] \quad (3.70)$$

$$PE_{L6} = m_6^L g \left[L_3 s\theta_3 + \frac{L_6}{2} s(\theta_{36}) \right] \quad (3.71)$$

$$PE_{L7} = m_7^L g [L_1 s\theta_1 + L_4 s\theta_{14} + g_7 s(\theta_1 + \theta_4 + \theta_7 + \beta)] \quad (3.72)$$

$$PE_{A1} = \frac{1}{2} K(\phi_1 - \theta_1)^2 \quad (3.73)$$

$$PE_{A2} = \frac{1}{2} K(\phi_2 - \theta_2)^2 \quad (3.74)$$

$$PE_{A3} = \frac{1}{2} K(\phi_3 - \theta_3)^2 \quad (3.75)$$

The total potential energy of the system is the sum of all potential energies of links and actuators.

$$\begin{aligned} U = & m_1^L g \frac{L_1}{2} s\theta_1 + m_2^L g \frac{L_2}{2} s\theta_2 + m_3^L g \frac{L_3}{2} s\theta_3 + m_4^L g \left[L_1 s\theta_1 + \frac{L_4}{2} s(\theta_{14}) \right] + \\ & m_5^L g \left[L_2 s\theta_2 + \frac{L_5}{2} s(\theta_{25}) \right] + m_6^L g \left[L_3 s\theta_3 + \frac{L_6}{2} s(\theta_{36}) \right] + m_7^L g [L_1 s\theta_1 + L_4 s\theta_{14} + \\ & g_7 s(\theta_1 + \theta_4 + \theta_7 + \beta)] + \frac{1}{2} K(\phi_1 - \theta_1)^2 + \frac{1}{2} K(\phi_2 - \theta_2)^2 + \\ & \frac{1}{2} K(\phi_3 - \theta_3)^2 \end{aligned} \quad (3.76)$$

The Lagrange components related to the total kinetic energy are given as bellow.

$$\begin{aligned} \frac{\partial U}{\partial \theta_1} = & m_1^L g \frac{L_1}{2} c\theta_1 + m_4^L g \left[L_1 c\theta_1 + \frac{L_4}{2} c(\theta_{14}) \right] + m_7^L g [L_1 c\theta_1 + L_4 c(\theta_{14}) + \\ & g_7 c(\theta_1 + \theta_4 + \theta_7 + \\ & \beta)] \end{aligned} \quad (3.77)$$

$$\frac{\partial U}{\partial \theta_2} = m_2^L g \frac{L_2}{2} c\theta_2 + m_5^L g [L_2 c\theta_2 + \frac{L_5}{2} c(\theta_{25})] \quad (3.78)$$

$$\frac{\partial U}{\partial \theta_3} = m_3^L g \frac{L_3}{2} c\theta_3 + m_6^L g [L_3 c\theta_3 + \frac{L_6}{2} c(\theta_{36})] \quad (3.79)$$

$$\frac{\partial U}{\partial \theta_4} = m_4^L g \frac{L_4}{2} c(\theta_{14}) + m_7^L g [L_4 c(\theta_{14}) + g_7 c(\theta_{147} + \beta)] \quad (3.80)$$

$$\frac{\partial U}{\partial \theta_5} = m_5^L g \frac{L_5}{2} c(\theta_{25}) \quad (3.81)$$

$$\frac{\partial U}{\partial \theta_5} = m_5^L g \frac{L_5}{2} c(\theta_{25}) \quad (3.82)$$

$$\frac{\partial U}{\partial \theta_7} = m_7^L g [g_7 c(\theta_{147} + \beta)] \quad (3.83)$$

$$\frac{\partial U}{\partial \phi_1} = K(\phi_1 - \theta_1) \quad (3.84)$$

$$\frac{\partial U}{\partial \phi_2} = K(\phi_2 - \theta_2) \quad (3.85)$$

$$\frac{\partial U}{\partial \phi_3} = K(\phi_3 - \theta_3) \quad (3.86)$$

3.1.3 Closed-Loop Constraint Equations

Disconnecting the system at H and I at Figure 3.2 gives four open kinematic chains which result in four constraint equations. Position level constraint equations may be formulated by re-connect the disconnected joints at H and I. this may be done according to the formula below.

$$\psi_i(\theta_1, \dots, \theta_m) = 0 \quad i = 1, \dots, (m - n) \quad (3.87)$$

$$L_1 c \theta_1 + L_4 c \theta_{14} + L_7 c \theta_{147} - L_2 c \theta_2 - L_5 c \theta_{25} - d_0 = 0 \quad (3.88)$$

$$L_1 s \theta_1 + L_4 s \theta_{14} + L_7 s \theta_{147} - L_2 s \theta_2 - L_5 s \theta_{25} = 0 \quad (3.88)$$

$$L_1 c \theta_1 + L_4 c \theta_{14} + d_7 c (\theta_{147} + \alpha) - L_3 c \theta_3 - L_6 c \theta_{36} = 0 \quad (3.89)$$

$$L_1 s \theta_1 + L_4 s \theta_{14} + d_7 s (\theta_{147} + \alpha) - L_3 s \theta_3 - L_6 s \theta_{36} = 0 \quad (3.90)$$

Differentiating the above equations gives the following.

$$-L_1 s \theta_1 \dot{\theta}_1 - L_4 s \theta_{14} \dot{\theta}_{14} - L_7 s \theta_{147} \dot{\theta}_{147} + L_2 s \theta_2 \dot{\theta}_2 + L_5 s \theta_{25} \dot{\theta}_{25} \quad (3.91)$$

$$L_1 c \theta_1 \dot{\theta}_1 + L_4 c \theta_{14} \dot{\theta}_{14} + L_7 c \theta_{147} \dot{\theta}_{147} - L_2 c \theta_2 \dot{\theta}_2 - L_5 c \theta_{25} \dot{\theta}_{25} \quad (3.92)$$

$$-L_1 s \theta_1 \dot{\theta}_1 - L_4 s \theta_{14} \dot{\theta}_{14} - d_7 s (\theta_7 + \alpha) (\dot{\theta}_7) + L_3 s \theta_3 \dot{\theta}_3 + L_6 s \theta_{36} (\dot{\theta}_{36}) \quad (3.93)$$

$$L_1 c \theta_1 \dot{\theta}_1 + L_4 c \theta_{14} \dot{\theta}_{14} + d_7 c (\theta_7 + \alpha) (\dot{\theta}_7) - L_3 c \theta_3 \dot{\theta}_3 - L_6 c \theta_{36} (\dot{\theta}_{36}) \quad (3.94)$$

The above equations may be written with symbols as follows.

$$B_{11} \dot{\theta}_1 + B_{12} \dot{\theta}_2 + B_{13} \dot{\theta}_3 + B_{14} \dot{\theta}_4 + B_{15} \dot{\theta}_5 + B_{16} \dot{\theta}_6 + B_{17} \dot{\theta}_7 \quad (3.95)$$

$$B_{21} \dot{\theta}_1 + B_{22} \dot{\theta}_2 + B_{23} \dot{\theta}_3 + B_{24} \dot{\theta}_4 + B_{25} \dot{\theta}_5 + B_{26} \dot{\theta}_6 + B_{27} \dot{\theta}_7 \quad (3.96)$$

$$B_{31} \dot{\theta}_1 + B_{32} \dot{\theta}_2 + B_{33} \dot{\theta}_3 + B_{34} \dot{\theta}_4 + B_{35} \dot{\theta}_5 + B_{36} \dot{\theta}_6 + B_{37} \dot{\theta}_7 \quad (3.97)$$

$$B_{41} \dot{\theta}_1 + B_{42} \dot{\theta}_2 + B_{43} \dot{\theta}_3 + B_{44} \dot{\theta}_4 + B_{45} \dot{\theta}_5 + B_{46} \dot{\theta}_6 + B_{47} \dot{\theta}_7 \quad (3.98)$$

where,

$$B_{11} = -L_1 s \theta_1 - L_4 s \theta_{14} - L_7 s \theta_{147} \quad (3.99)$$

$$B_{12} = L_2 s \theta_2 + L_5 s \theta_{25} \quad (3.100)$$

$$B_{13} = 0 \quad (3.101)$$

$$B_{14} = -L_4 s \theta_{14} - L_7 s \theta_{147} \quad (3.102)$$

$$B_{15} = L_5 s \theta_{25} \quad (3.103)$$

$$B_{16} = 0 \quad (3.104)$$

$$B_{17} = -L_7 s \theta_{147} \quad (3.105)$$

$$B_{21} = L_1 c \theta_1 + L_4 c \theta_{14} + L_7 c \theta_{147} \quad (3.106)$$

$$B_{22} = -L_2 c \theta_2 - L_5 c \theta_{25} \quad (3.107)$$

$$B_{23} = 0 \quad (3.108)$$

$$B_{24} = L_4 c \theta_{14} + L_7 c \theta_{147} \quad (3.109)$$

$$B_{25} = -L_5 c \theta_{25} \quad (3.110)$$

$$B_{26} = 0 \quad (3.111)$$

$$B_{27} = L_7 c \theta_{147} \quad (3.112)$$

$$B_{31} = -L_1 s \theta_1 - L_4 s \theta_{14} - d_7 s (\theta_{147} + \alpha) \quad (3.113)$$

$$B_{32} = 0 \quad (3.114)$$

$$B_{33} = L_3 s \theta_3 + L_6 s \theta_{36} \quad (3.115)$$

$$B_{34} = -L_4 s \theta_{14} - d_7 s (\theta_{147} + \alpha) \quad (3.116)$$

$$B_{35} = 0 \quad (3.117)$$

$$B_{36} = L_6 s \theta_{36} \quad (3.118)$$

$$B_{37} = -d_7 s (\theta_{147} + \alpha) \quad (3.119)$$

$$B_{41} = L_1 c \theta_1 + L_4 c \theta_{14} + d_7 c (\theta_{147} + \alpha) \quad (3.120)$$

$$B_{42} = 0 \quad (3.121)$$

$$B_{43} = -L_3 c \theta_3 - L_6 c \theta_{36} \quad (3.122)$$

$$B_{44} = L_4 c \theta_{14} + d_7 c (\theta_{147} + \alpha) \quad (3.123)$$

$$B_{45} = 0 \quad (3.124)$$

$$B_{46} = -L_6 c \theta_{36} \quad (3.125)$$

$$B_{47} = d_7 c (\theta_{147} + \alpha) \quad (3.126)$$

Separating the non-actuated joint variables gives.

$$\begin{bmatrix} \dot{\theta}_4 \\ \dot{\theta}_5 \\ \dot{\theta}_6 \\ \dot{\theta}_7 \end{bmatrix} = - \begin{bmatrix} B_{14} & B_{15} & B_{16} & B_{17} \\ B_{24} & B_{25} & B_{26} & B_{27} \\ B_{34} & B_{35} & B_{36} & B_{37} \\ B_{44} & B_{45} & B_{46} & B_{47} \end{bmatrix}^{-1} \begin{bmatrix} B_{11} & B_{12} & B_{13} \\ B_{21} & B_{22} & B_{23} \\ B_{31} & B_{32} & B_{33} \\ B_{41} & B_{42} & B_{43} \end{bmatrix} \begin{bmatrix} \dot{\theta}_1 \\ \dot{\theta}_2 \\ \dot{\theta}_3 \end{bmatrix} \quad (3.127)$$

As a result,

$$\dot{\theta}_{4 \times 1}^u = \hat{C}_{4 \times 3} \dot{q}_{3 \times 1} \quad (3.128)$$

One can write the constraint matrix B as follows.

$$\hat{B}^T = \begin{bmatrix} B_{11} & B_{21} & B_{31} & B_{41} \\ B_{12} & B_{22} & B_{32} & B_{42} \\ B_{13} & B_{23} & B_{33} & B_{43} \\ B_{14} & B_{24} & B_{34} & B_{44} \\ B_{15} & B_{25} & B_{35} & B_{45} \\ B_{16} & B_{26} & B_{36} & B_{46} \\ B_{17} & B_{27} & B_{37} & B_{47} \end{bmatrix} \quad (3.129)$$

where,

$$\hat{B}^a = \begin{bmatrix} B_{11} & B_{12} & B_{13} \\ B_{21} & B_{22} & B_{23} \\ B_{31} & B_{32} & B_{33} \end{bmatrix} \quad (3.130)$$

and

$$\hat{B}^u = \begin{bmatrix} B_{14} & B_{15} & B_{16} & B_{17} \\ B_{24} & B_{25} & B_{26} & B_{27} \\ B_{34} & B_{35} & B_{36} & B_{37} \\ B_{44} & B_{45} & B_{46} & B_{47} \end{bmatrix} \quad (3.131)$$

The end-effector position and orientation can be written as follows.

$$\begin{bmatrix} x_1 \\ x_2 \\ x_3 \end{bmatrix} = \begin{bmatrix} (L_1 c \theta_1 + L_4 c \theta_{14} + d_7 c(\theta_{147} + \alpha)) \\ (L_1 s \theta_1 + L_4 s \theta_{14} + d_7 s(\theta_{147} + \alpha)) \\ \theta_{147} \end{bmatrix} \quad (3.132)$$

Where x_1 and x_2 stand for the position of the end-effector in the x -direction and the y -direction respectively and x_3 stands for the orientation of the end-effector.

3.1.4 System Equations of Motion

Corresponding to the vector of the robot joint variables of the rigid links from Equation 2.1, one can write in matrix form the following system equations of motion.

$$\begin{bmatrix} M_{11} & 0 & 0 & M_{14} & 0 & 0 & M_{17} \\ 0 & M_{22} & 0 & 0 & M_{25} & 0 & 0 \\ 0 & 0 & M_{33} & 0 & 0 & M_{36} & 0 \\ M_{14} & 0 & 0 & M_{44} & 0 & 0 & M_{47} \\ 0 & M_{25} & 0 & 0 & M_{55} & 0 & 0 \\ 0 & 0 & M_{36} & 0 & 0 & M_{66} & 0 \\ M_{17} & 0 & 0 & M_{47} & 0 & 0 & M_{77} \end{bmatrix} \begin{bmatrix} \ddot{\theta}_1 \\ \ddot{\theta}_2 \\ \ddot{\theta}_3 \\ \ddot{\theta}_4 \\ \ddot{\theta}_5 \\ \ddot{\theta}_6 \\ \ddot{\theta}_7 \end{bmatrix} + \begin{bmatrix} Q_1 \\ Q_2 \\ Q_3 \\ Q_4 \\ Q_5 \\ Q_6 \\ Q_7 \end{bmatrix} + \hat{B}^T \lambda = 0 \quad (3.133)$$

Where,

$$\begin{aligned} M_{11} = & \left[m_1^L \frac{L_1^2}{4} + I_{1zz} \right] + M_4^L L_1^2 + M_4^L L_1 L_4 c \theta_4 + \left[M_4^L \frac{L_4^2}{4} + I_{4zz} \right] + m_7^L L_4^2 \\ & + [m_7^L g_7^2 + I_{7zz}] + 2m_7^L L_1 L_4 c \theta_4 + 2m_7^L L_1 g_7 c(\theta_4 + \theta_7 + \beta) \\ & + 2m_7^L L_4 g_7 c(\theta_7 + \beta) \end{aligned} \quad (3.134)$$

$$M_{14} = \frac{1}{2} M_4^L L_1 L_4 c \theta_4 + \left[m_4^L \frac{L_4^2}{4} + I_{4zz} \right] + m_7^L L_4^2 + [m_7^L g_7^2 + I_{7zz}] + m_7^L L_1 L_4 c \theta_4 + m_7^L L_1 g_7 c(\theta_4 + \theta_7 + \beta) + 2m_7^L L_4 g_7 c(\theta_7 + \beta) \quad (3.135)$$

$$M_{17} = [m_7^L g_7^2 + I_{7zz}] + m_7^L L_1 g_7 c(\theta_4 + \theta_7 + \beta) + m_7^L L_4 g_7 c(\theta_7 + \beta) \quad (3.136)$$

$$M_{22} = \left[m_2^L \frac{L_2^2}{4} + I_{2zz} \right] + m_5^L L_2^2 + m_5^L L_2 L_5 c \theta_5 + \left[m_5^L \frac{L_5^2}{4} + I_{5zz} \right] \quad (3.137)$$

$$M_{25} = \frac{1}{2} m_5^L L_2 L_5 c \theta_5 + \left[m_5^L \frac{L_5^2}{4} + I_{5zz} \right] \quad (3.138)$$

$$M_{33} = \left[m_3^L \frac{L_3^2}{4} + I_{3zz} \right] + m_6^L L_3^2 + m_6^L L_3 L_6 c \theta_6 + \left[m_6^L \frac{L_6^2}{4} + I_{6zz} \right] \quad (3.139)$$

$$M_{36} = \frac{1}{2} m_6^L L_3 L_6 c \theta_6 + \left[m_6^L \frac{L_6^2}{4} + I_{6zz} \right] \quad (3.140)$$

$$M_{44} = \left[m_4^L \frac{L_4^2}{4} + I_{4zz} \right] + m_7^L L_4^2 + [m_7^L g_7^2 + I_{7zz}] + 2m_7^L L_4 g_7 c(\theta_7 + \beta) \quad (3.141)$$

$$M_{47} = [m_7^L g_7^2 + I_{7zz}] + m_7^L L_4 g_7 c(\theta_7 + \beta) \quad (3.142)$$

$$M_{55} = m_5^L \frac{L_5^2}{4} + I_{5zz} \quad (3.143)$$

$$M_{66} = m_6^L \frac{L_6^2}{4} + I_{6zz} \quad (3.144)$$

$$M_{77} = m_7^L g_7^2 + I_{7zz} \quad (3.145)$$

$$Q_1 = -m_4^L L_1 L_4 s \theta_4 \dot{\theta}_1 \dot{\theta}_4 - \frac{1}{2} m_4^L L_1 L_4 s \theta_4 \dot{\theta}_4^2 - 2m_7^L L_1 L_4 s \theta_4 \dot{\theta}_1 \dot{\theta}_4 - m_7^L L_1 L_4 s \theta_4 \dot{\theta}_4^2 - 2m_7^L L_1 g_7 L_1 s(\theta_4 + \theta_7 + \beta) \dot{\theta}_1 \dot{\theta}_7 - 2m_7^L L_1 g_7 L_1 s(\theta_4 + \theta_7 + \beta) \dot{\theta}_4 \dot{\theta}_7 - m_7^L L_1 g_7 s(\theta_4 + \theta_7 + \beta) \dot{\theta}_4^2 - m_7^L L_1 g_7 s(\theta_4 + \theta_7 + \beta) \dot{\theta}_4 \dot{\theta}_7 - m_7^L L_1 g_7 s(\theta_4 + \theta_7 + \beta) \dot{\theta}_4 \dot{\theta}_7 - m_7^L L_1 g_7 s(\theta_4 + \theta_7 + \beta) \dot{\theta}_7^2 - 2m_7^L L_4 g_7 s(\theta_7 + \beta) \dot{\theta}_1 \dot{\theta}_7 - m_7^L L_4 g_7 s(\theta_7 + \beta) \dot{\theta}_4 \dot{\theta}_7 - m_7^L L_4 g_7 s(\theta_7 + \beta) \dot{\theta}_7^2 - m_7^L L_4 g_7 s(\theta_7 + \beta) \dot{\theta}_4 \dot{\theta}_7 + m_1^L g \frac{L_1}{2} c \theta_1 + m_4^L g \left[L_1 c \theta_1 + \frac{L_4}{2} c(\theta_{14}) \right] + m_7^L g [L_1 c \theta_1 + L_4 c(\theta_{14})] + g_7 c(\theta_{147} + \beta) \quad (3.146)$$

$$Q_2 = -m_5^L L_2 L_5 s \theta_5 \dot{\theta}_2 \dot{\theta}_5 - \frac{1}{2} m_5^L L_2 L_5 s \theta_5 \dot{\theta}_5^2 + m_2^L g \frac{L_2}{2} c \theta_2 + m_5^L g [L_2 c \theta_2 + \frac{L_5}{2} c(\theta_2 + \theta_5)] \quad (3.147)$$

$$Q_3 = -m_6^L L_3 L_6 s \theta_6 \dot{\theta}_3 \dot{\theta}_6 - \frac{1}{2} m_6^L L_3 L_6 s \theta_6 \dot{\theta}_6^2 + m_3^L g \frac{L_3}{2} c \theta_3 + m_6^L g [L_3 c \theta_3 + \frac{L_6}{2} c(\theta_3 + \theta_6)] \quad (3.148)$$

$$Q_4 = [-m_7^L L_4 g_7 s(\theta_7 + \beta) - m_7^L L_4 g_7 s(\theta_7 + \beta)] \dot{\theta}_1 \dot{\theta}_7 + [-2m_7^L L_4 g_7 s(\theta_7 + \beta)] \dot{\theta}_4 \dot{\theta}_7 + [-m_7^L L_4 g_7 s(\theta_7 + \beta)] \dot{\theta}_7^2 + [m_4^L L_1 L_4 s \theta_4 + 2m_7^L L_1 L_4 s \theta_4 + 2m_7^L L_1 g_7 s(\theta_4 + \theta_7 + \beta)] \frac{1}{2} \dot{\theta}_1^2 + m_4^L g \frac{L_4}{4} c \theta_{14} + m_7^L [L_4 c \theta_{14} + g_7 c(\theta_{147} + \beta)] \quad (3.149)$$

$$Q_5 = \frac{1}{2} \dot{\theta}_2^2 [m_5^L L_2 L_5 s \theta_5] + m_5^L g \frac{L_5}{2} c \theta_{25} \quad (3.150)$$

$$Q_6 = \frac{1}{2} \dot{\theta}_3^2 [m_6^L L_3 L_6 s \theta_6] + m_6^L g \frac{L_6}{2} c \theta_{36} \quad (3.151)$$

$$Q_7 = [m_7^L L_1 g_7 s(\theta_{47} + \beta) + m_7^L L - 4 g_7 s(\theta_7 + \beta)] \dot{\theta}_2^2 + [m_7^L L_4 g_7 s(\theta_7 + \beta)] \dot{\theta}_4^2 + [2m_7^L L_4 g_7 s(\theta_7 + \beta)] \dot{\theta}_1 \dot{\theta}_4 + [g_7 c(\theta_{147} + \beta)] m_7^L g \quad (3.152)$$

Corresponding to the vector of the actuator joint variables from Equation 2.2, one can write in matrix form the following system equations of motion.

$$\begin{bmatrix} I_{11} & 0 & 0 \\ 0 & I_{22} & 0 \\ 0 & 0 & I_{33} \end{bmatrix} \begin{bmatrix} \ddot{\phi}_1 \\ \ddot{\phi}_2 \\ \ddot{\phi}_3 \end{bmatrix} - \begin{bmatrix} K_1(\theta_1 - \phi_1) \\ K_2(\theta_2 - \phi_2) \\ K_3(\theta_3 - \phi_3) \end{bmatrix} = \begin{bmatrix} T_1 \\ T_2 \\ T_3 \end{bmatrix} \quad (3.153)$$

It is wished for writing Equation 3.133 in only terms of actuated joint variables, this may be done by first writing the above mentioned equation in two parts as below.

$$\hat{M}^{aa}\ddot{\bar{q}} + \hat{M}^{au}\ddot{\bar{\theta}}^u + \bar{Q}^a + \hat{K}(\bar{q} - \bar{\phi}) - \hat{B}^{aT}\bar{\lambda} = 0 \quad (3.154)$$

$$\hat{M}^{auT} + \hat{M}^{uu}\ddot{\bar{\theta}}^u + \bar{Q}^u - \hat{B}^{uT}\bar{\lambda} = 0 \quad (3.155)$$

where,

$\hat{K} = \text{diag}[K_i]$ for $i = 1, 2, 3$.

$$\hat{M}^{aa} = \begin{bmatrix} M_{11} & 0 & 0 \\ 0 & M_{22} & 0 \\ 0 & 0 & M_{33} \end{bmatrix} \quad (3.156)$$

$$\hat{M}^{au} = \begin{bmatrix} M_{14} & 0 & 0 & M_{17} \\ 0 & M_{25} & 0 & 0 \\ 0 & 0 & M_{36} & 0 \end{bmatrix} \quad (3.157)$$

$$\hat{M}^{uu} = \begin{bmatrix} M_{44} & 0 & 0 & M_{77} \\ 0 & M_{55} & 0 & 0 \\ M_{47} & 0 & 0 & M_{77} \end{bmatrix} \quad (3.158)$$

$$\bar{Q}^{aT} = [Q_1 \quad Q_2 \quad Q_3] \quad (3.159)$$

$$\bar{Q}^{uT} = [Q_4 \quad Q_5 \quad Q_6 \quad Q_7] \quad (3.160)$$

In order to eliminate the non-actuated joint variables, Equation 2.15 and 2.17 will be used, after that, Equation 3.153 will be solved for λ and then it will be substituted in Equation 3.152 gives.

$$\hat{M}^*\ddot{\bar{q}} + \bar{Q}^* + \hat{K}(\bar{q} - \bar{\phi}) = 0 \quad (3.161)$$

Where,

$$\hat{M}^* = [\hat{M}^{aa} - \hat{M}^{au}\hat{B}^{u-1}\hat{B}^a] - \hat{B}^{aT}(\hat{B}^{u-1})[\hat{M}^{auT} - \hat{M}^{uu}\hat{B}^{u-1}\hat{B}^u] \quad (3.162)$$

$$Q^* =$$

$$\begin{aligned} & [-\hat{M}^{au}\hat{B}^{u-1}\dot{\hat{B}}^a + \hat{B}^{aT}(\hat{B}^{u-1})^T\hat{M}^{uu}\hat{B}^{u-1}\dot{\hat{B}}^a]\dot{\bar{q}} + \\ & [-\hat{M}^{au}\hat{B}^{u-1}\dot{\hat{B}}^u + \hat{B}^{aT}(\hat{B}^{u-1})^T\hat{M}^{uu}\hat{B}^{u-1}\dot{\hat{B}}^u]\dot{\bar{\theta}}^u + \bar{Q}^a - \hat{B}^{aT}(\hat{B}^{u-1})^T\bar{Q}^u \end{aligned} \quad (3.163)$$

3.2 Control Simulation and Results

The execution of the control law is tested by using MATLAB® software. All the constants and the variables of the system are presented and an m-file program is written to carries out the procedures to calculate the control torques at each decided time step.

The early mentioned control algorithm in Chapter 2 will be exercised together with the implicit numerical integration method to find the control torques exactly as mentioned before and the procedure will be as follows.

The nonlinear algebraic equation 2.46 will be solved by functional iteration. For this purpose, using Equation 2.48, Equation 2.43, Equation 2.25, Equation 2.46 is written in the following form

$$\begin{aligned} \ddot{q}_{k+1} = & \left(\hat{f} \frac{1}{h} + \dot{\hat{f}} + \hat{C}_1 \hat{f} + \hat{C}_2 h \hat{f} + \hat{C}_3 h^2 \hat{f} + \hat{C}_4 h^3 \hat{f} \right)^{-1} \times \left\{ \hat{f} \frac{1}{h} \dot{q}_k + \bar{z}_a + \dot{\bar{z}}_a (t_{k+1} - t_a) + \right. \\ & \ddot{x}_{k+1}^d - \ddot{x}_a^d - \ddot{x}_a^d (t_{k+1} - t_a) + \hat{C}_1 [(\dot{x}_{k+1}^d - \dot{x}_k) - (\dot{x}_a^d - \dot{x}_a) - (\ddot{x}_a^d - \ddot{x}_a)(t_{k+1} - t_a)] + \\ & \hat{C}_2 [(\bar{x}_{k+1}^d - \bar{x}_k) - (\bar{x}_a^d - \bar{x}_a) - (\dot{x}_a^d - \dot{x}_a)(t_{k+1} - t_a)] - \hat{C}_3 (\bar{x}_a^d - \bar{x}_a)(t_{k+1} - t_a) + \\ & \left. \hat{C}_3 (h \bar{x}_{k+1}^d - h \bar{x}_k + \dot{\bar{\omega}}_k) + \hat{C}_4 (h^2 \bar{x}_{k+1}^d - h^2 \bar{x}_k + \dot{\bar{\omega}}_k h + \bar{\omega}_k) \right\} \quad (3.164) \end{aligned}$$

In the right hand side, beginning with \ddot{q}_k for \ddot{q}_{k+1} , after that, Equation 2.164 will be solved for the new value of \ddot{q}_{k+1} at the left hand side. Iteration lasts till the norm of difference between any two sequent iterations is minimal than a small number η . The simulation shows that for $\eta = 10^{-6}$, maximum three iterations are necessary. After finding the control torques they will be applied to the actual system expressed below to find the actual acceleration which will be numerically integrated to find the new joint and rotor velocities and positions to be used for the next time step.

$$\begin{bmatrix} \widehat{M}^* & 0 & 0 \\ 0 & \widehat{I}^r & -I \\ \widehat{J} & 0 & 0 \end{bmatrix} \begin{bmatrix} \ddot{\bar{q}} \\ \ddot{\bar{\phi}} \\ \ddot{\bar{T}} \end{bmatrix} = \begin{bmatrix} -\bar{Q}^* - \widehat{K}(\bar{q} - \bar{\phi}) \\ \widehat{K}(\bar{q} - \bar{\phi}) \\ -\widehat{J}\dot{\bar{q}} + \ddot{x} \end{bmatrix} \quad (3.165)$$

The performance of the control law will be tested for three groups of simulation. First group is held with initial error and constant deployment motion stated as

$$\begin{bmatrix} x_1 \\ x_2 \\ x_3 \end{bmatrix} = \begin{bmatrix} x_p^d \\ y_p^d \\ \sigma^d \end{bmatrix} = \begin{bmatrix} 1.8m \\ 1.3m \\ 20deg \end{bmatrix}. \text{Second group is tested with initial error and without modeling}$$

error while the third group is tested with initial and modeling error. Modeling error is regarded by setting the robot mass and inertia properties and the torsional constants to be 20% smaller in the model.

The mass and geometric data, gear ratios and inertial properties utilized in the simulation are given in Table 1 and Table 2.

Symbol	Value	Symbol	Value
L_1	1.0m	L_7	1.0m
L_2	1.0m	d_7	0.57735m
L_3	1.0m	g_7	0.57735m
L_4	1.0m	d_0	3.0m
L_5	1.0m	α	30 deg.
L_6	1.0m	β	60 deg.

Table 1 Geometric Data

Symbol	Value	Symbol	Value
m_1^L	10 kg	m_2^A	1.2 kg
m_2^L	10 kg	m_3^A	1.2 kg
m_3^L	10 kg	I_{1zz}^r	$8 \times 10^{-5} kg.m^2$
m_4^L	10 kg	I_{2zz}^r	$8 \times 10^{-5} kg.m^2$
m_5^L	10 kg	I_{3zz}^r	$8 \times 10^{-5} kg.m^2$
m_6^L	10 kg	r_1	100
m_7^L	15 kg	r_2	100
m_1^A	1.2 kg	r_3	100

Table 2 Inertial, mass properties and Gear Ratios

The system is initially at rest with the following active joint positions.

$$\theta_{1_0} = 84^0 \quad (3.164)$$

$$\theta_{2_0} = 167^0 \quad (3.165)$$

$$\theta_{3_0} = 203^0 \quad (3.166)$$

This gives the following initial position of the end-effector.

$$x_{p_0} = 1.5789 \text{ m} \quad (3.167)$$

$$y_{p_0} = 1.5081 \text{ m} \quad (3.168)$$

$$\sigma_{p_0} = 0^0 \quad (3.169)$$

The desired motion trajectories are presented as follows.

$$x_p^d = \begin{cases} 1.62 + \frac{0.5}{T} \left[t - \frac{T}{2\pi} \sin \frac{2\pi t}{T} \right] m & 0 \leq t \leq T \\ 2.12m & t > T \end{cases} \quad (3.170)$$

$$y_p^d = \begin{cases} 1.45 - \frac{0.5}{T} \left[t - \frac{T}{2\pi} \sin \frac{2\pi t}{T} \right] m & 0 \leq t \leq T \\ 0.95m & t > T \end{cases} \quad (3.171)$$

$$\sigma^d = \begin{cases} 5 + \frac{20}{T} \left[t - \frac{T}{2\pi} \sin \frac{2\pi t}{T} \right] \text{deg.} & 0 \leq t \leq T \\ 25\text{deg.} & t > T \end{cases} \quad (3.172)$$

where, $T = 0.5\text{s}$ is the period of deployment motion and $t = 0.75\text{s}$ is the full time of simulation.

It is assumed that, during the path of the desired motion there will be no singular positions and it's also proved practically during the simulation.

The sampling time interval is set to be $h = 0.002$. Each group of simulation is held first with $\omega_i = 20 \text{ rad/s}$ for $i = 1, 2, 3$ and then with $\omega_i = 30 \text{ rad/s}$ for $i = 1, 2, 3$.

Results are presented as below.

First Group of Simulations

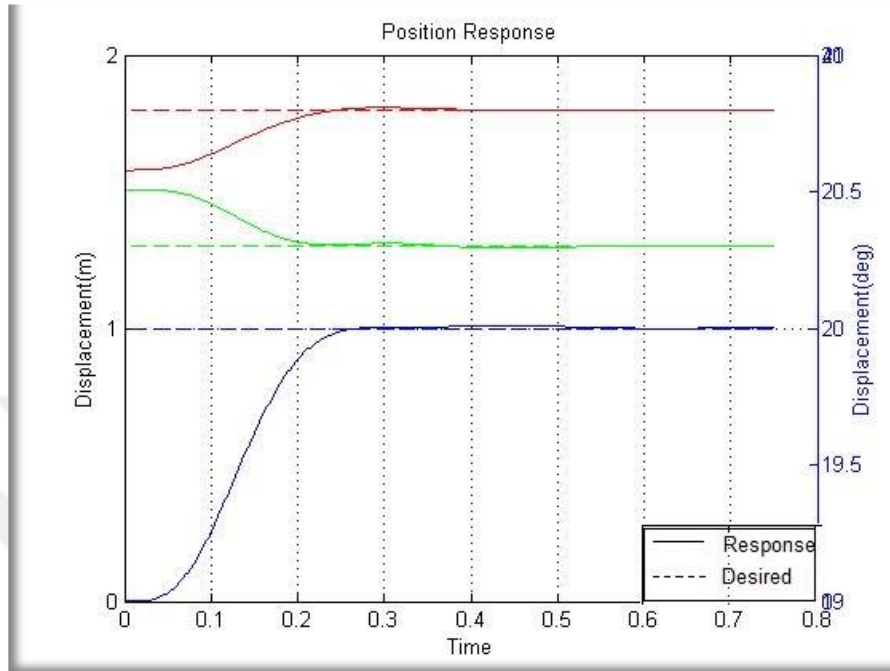


Figure 5 Position Response 1. x_1 , 2. x_2 , 3. x_3 (First Group $\omega_i = 20\text{rad/s}$)

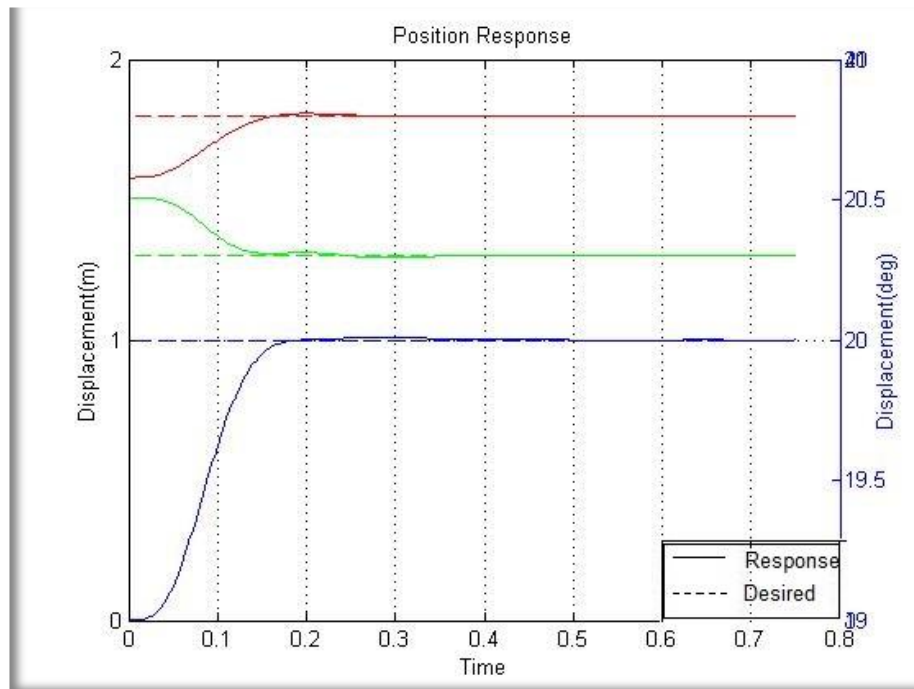


Figure 6 Position Response 1. x_1 , 2. x_2 , 3. x_3 (First Group $\omega_i = 30\text{rad/s}$)

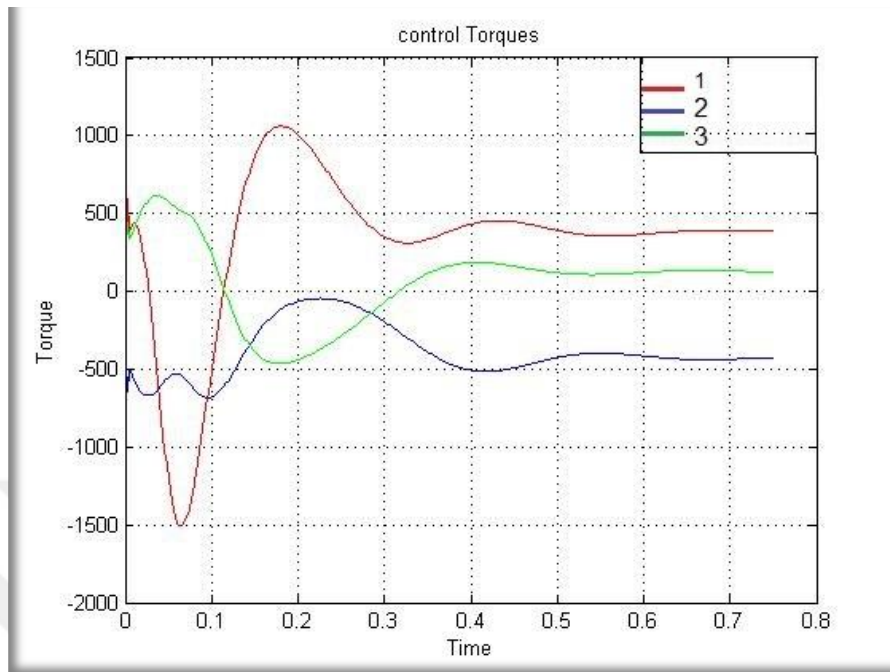


Figure 7 Control Torques 1. T_1^a , 2. T_2^a , 3. T_3^a (First Group $\omega_i = 20 \text{ rad/s}$)

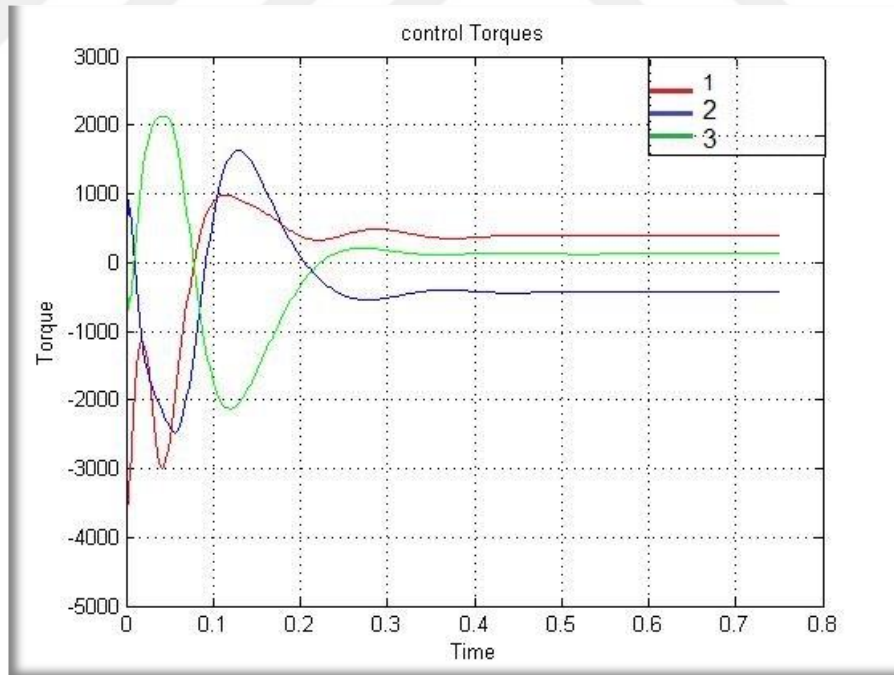


Figure 8 Control Torques 1. T_1^a , 2. T_2^a , 3. T_3^a (First Group $\omega_i = 30 \text{ rad/s}$)

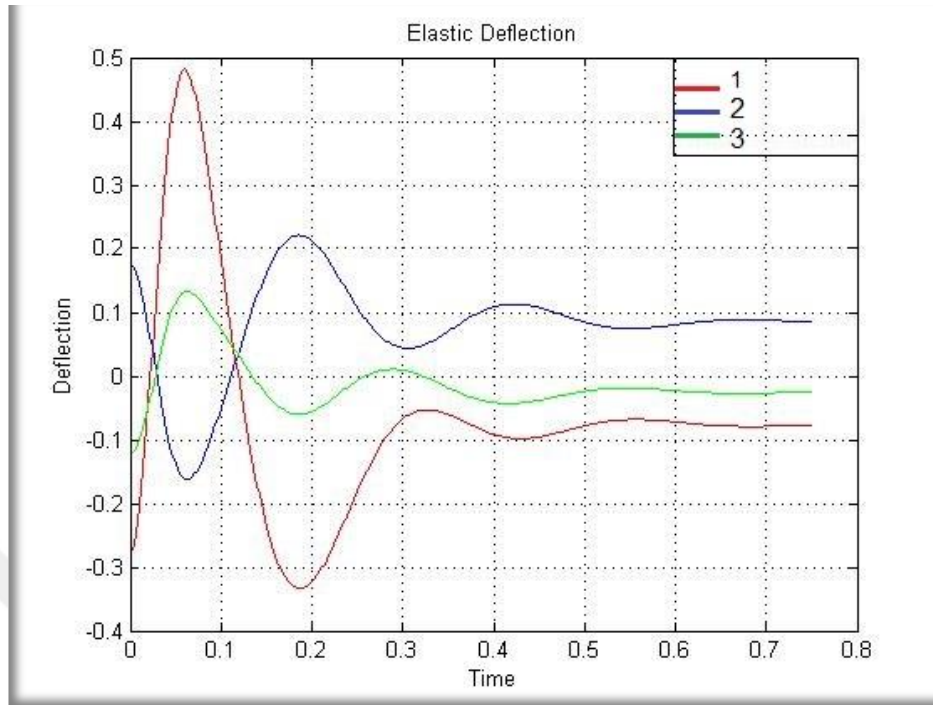


Figure 9 Deflections 1. $\theta_1 - \phi_1$, 2. $\theta_2 - \phi_2$, 3. $\theta_3 - \phi_3$ (First Group $\omega_i = 20 \text{ rad/s}$)

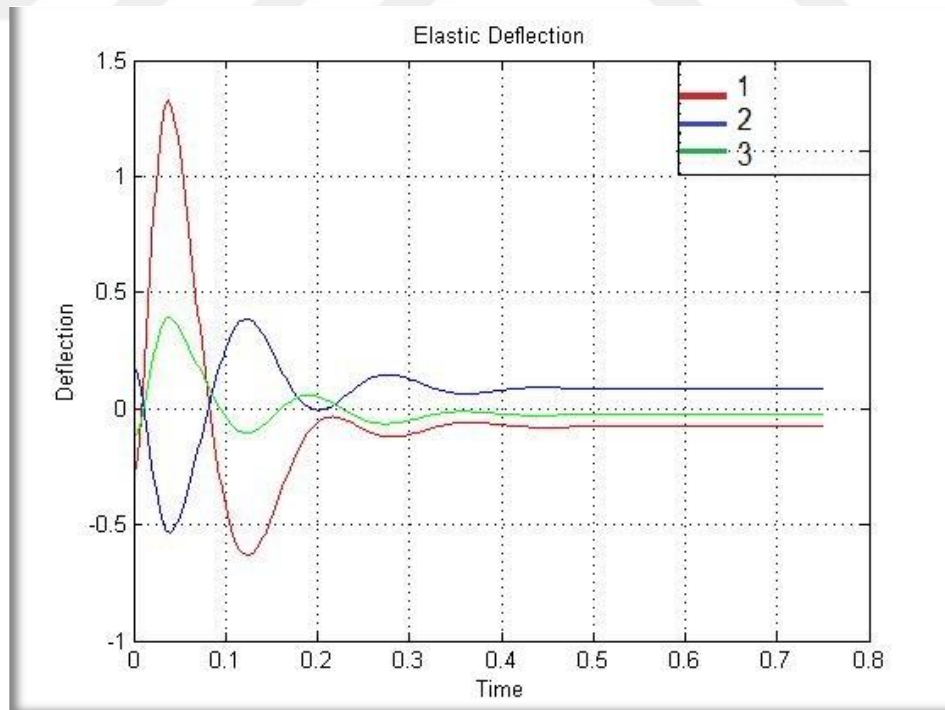


Figure 10 Deflections 1. $\theta_1 - \phi_1$, 2. $\theta_2 - \phi_2$, 3. $\theta_3 - \phi_3$ (First Group $\omega_i = 30 \text{ rad/s}$)

Second Group of Simulations

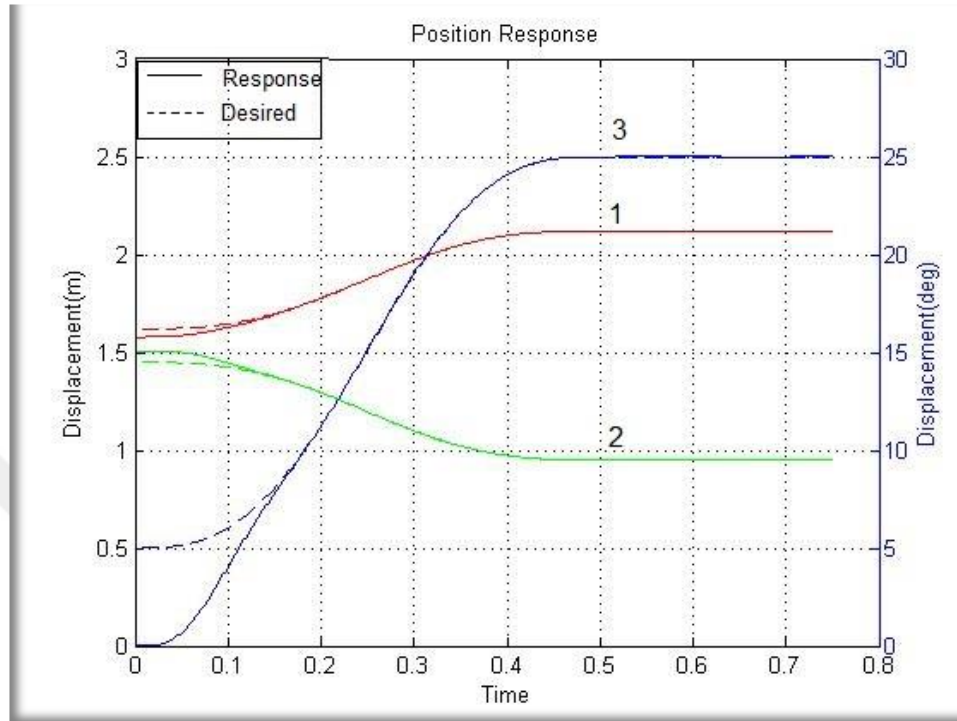


Figure 11 Position Response 1. x_1 , 2. x_2 , 3. x_3 (Second Group $\omega_i = 20\text{rad/s}$)

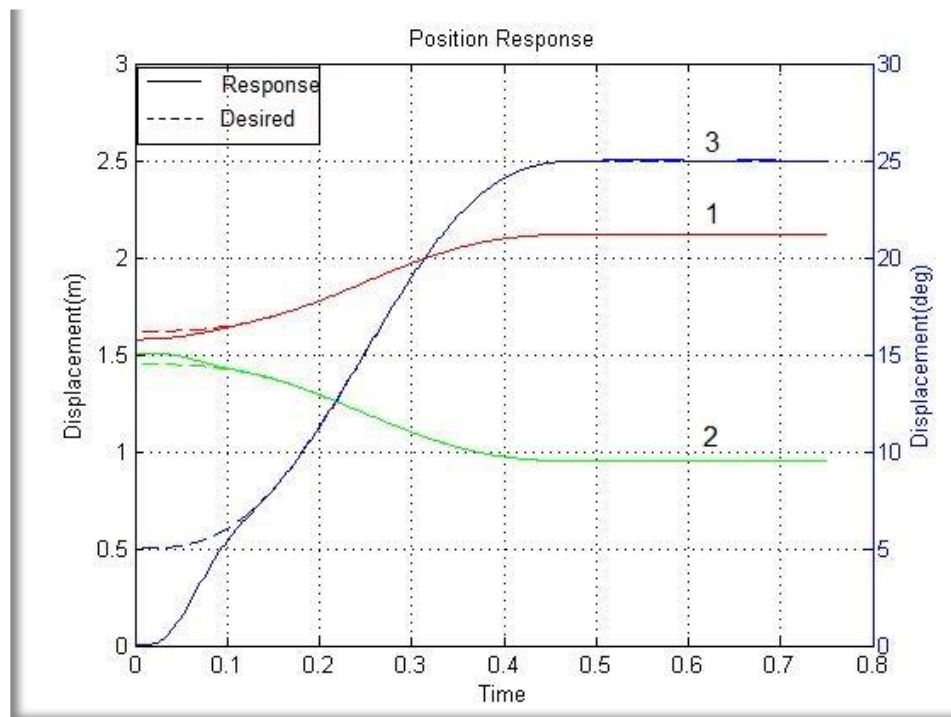


Figure 12 Position Response 1. x_1 , 2. x_2 , 3. x_3 (Second Group $\omega_i = 30\text{rad/s}$)

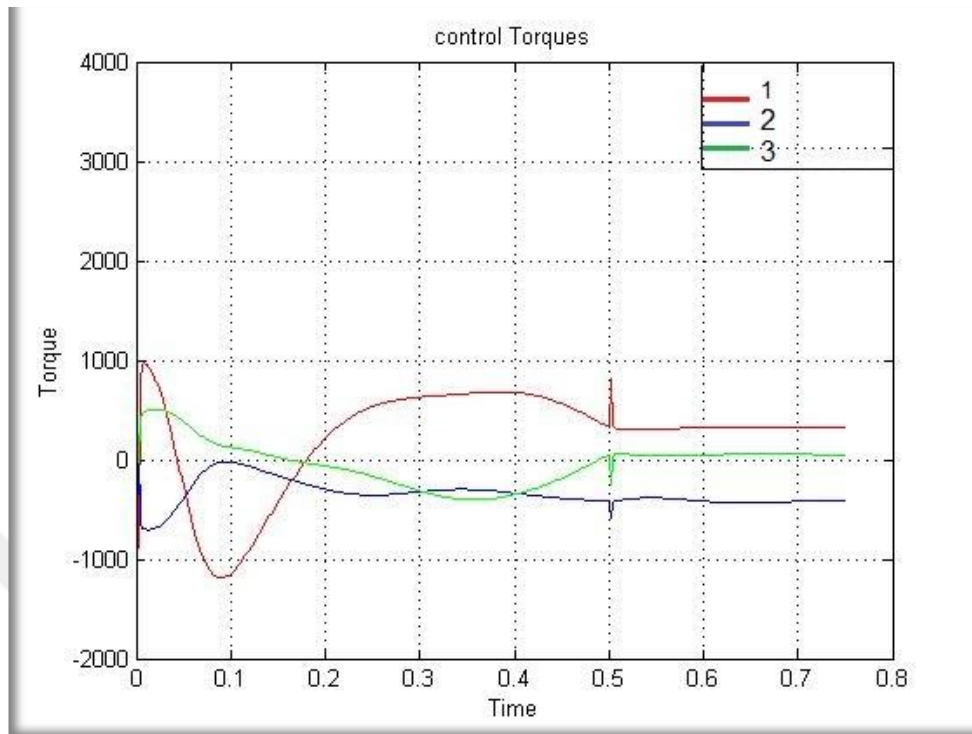


Figure 13 Control Torques 1. T_1^a , 2. T_2^a , 3. T_3^a (Second Group $\omega_i = 20 \text{ rad/s}$)

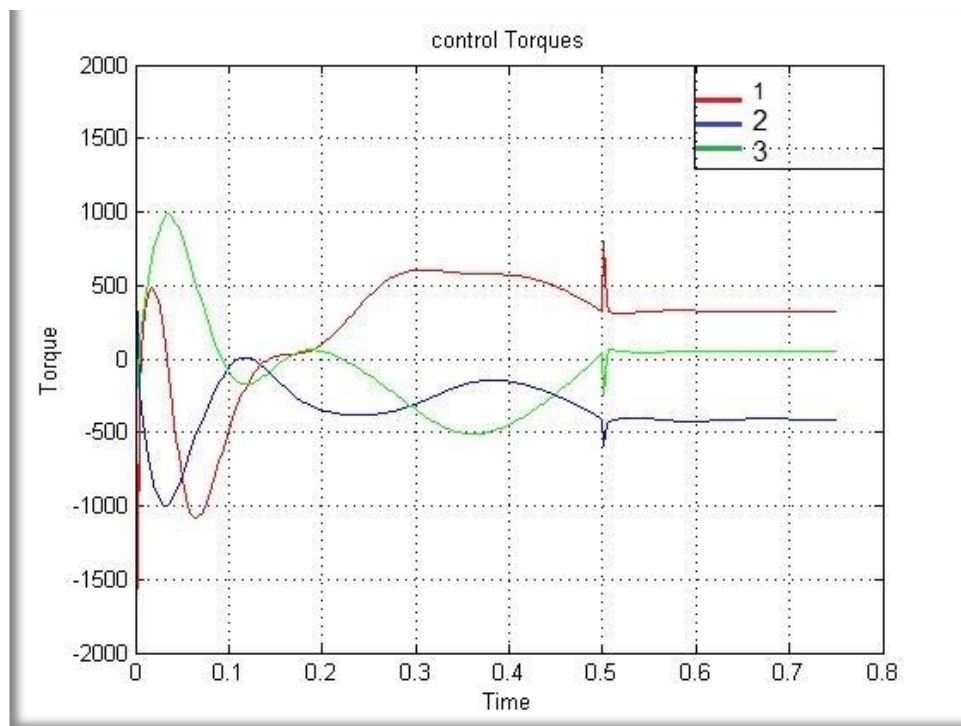


Figure 14 Control Torques 1. T_1^a , 2. T_2^a , 3. T_3^a (Second Group $\omega_i = 30 \text{ rad/s}$)

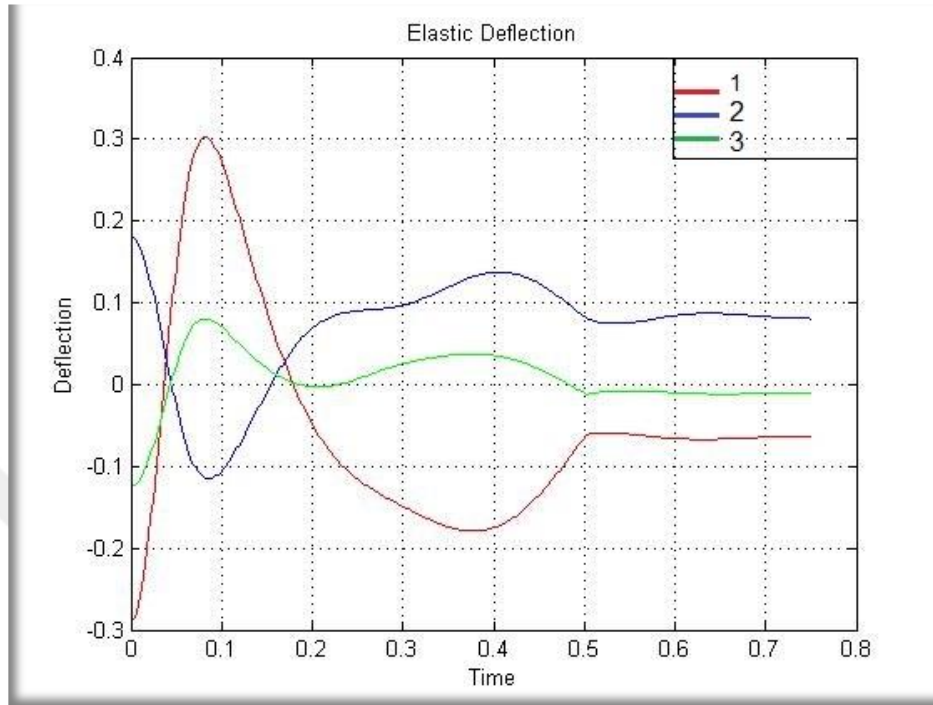


Figure 15 Deflections 1. $\theta_1 - \phi_1$, 2. $\theta_2 - \phi_2$, 3. $\theta_3 - \phi_3$ (Second Group $\omega_i = 20 \text{ rad/s}$)

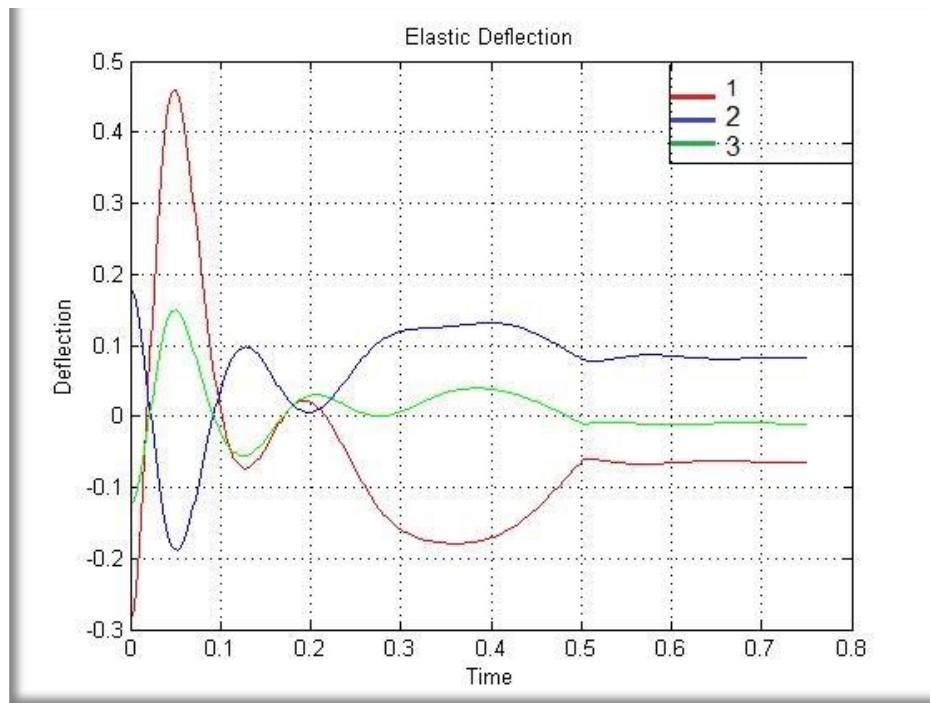


Figure 16 Deflections 1. $\theta_1 - \phi_1$, 2. $\theta_2 - \phi_2$, 3. $\theta_3 - \phi_3$ (Second Group $\omega_i = 30 \text{ rad/s}$)

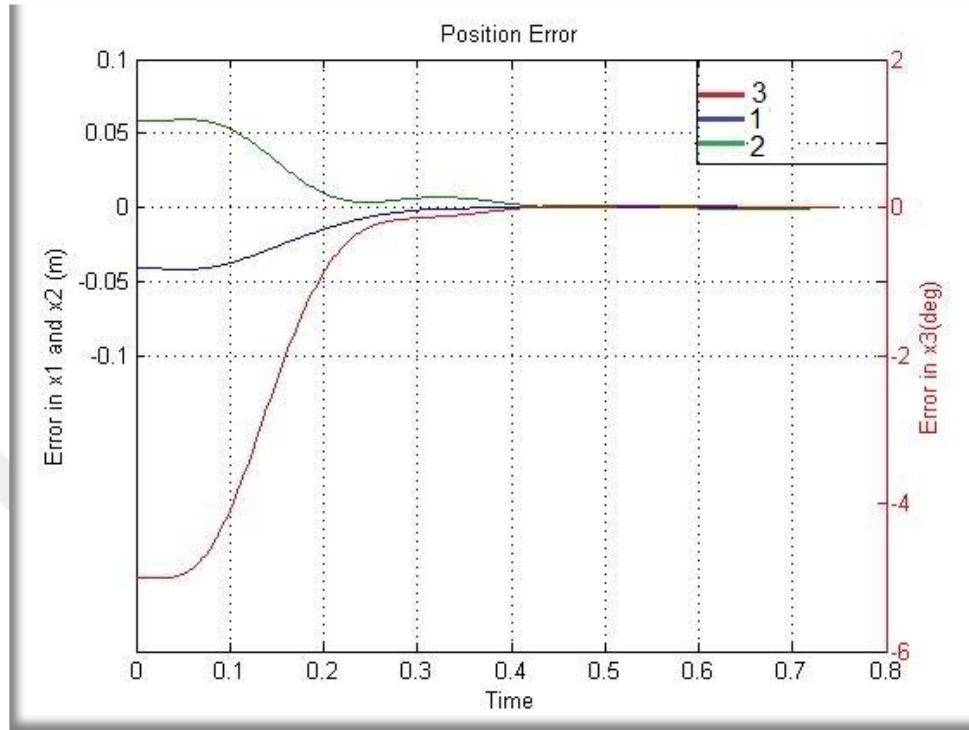


Figure 17 Position Errors (Second Group $\omega_i = 20 \text{ rad/s}$)

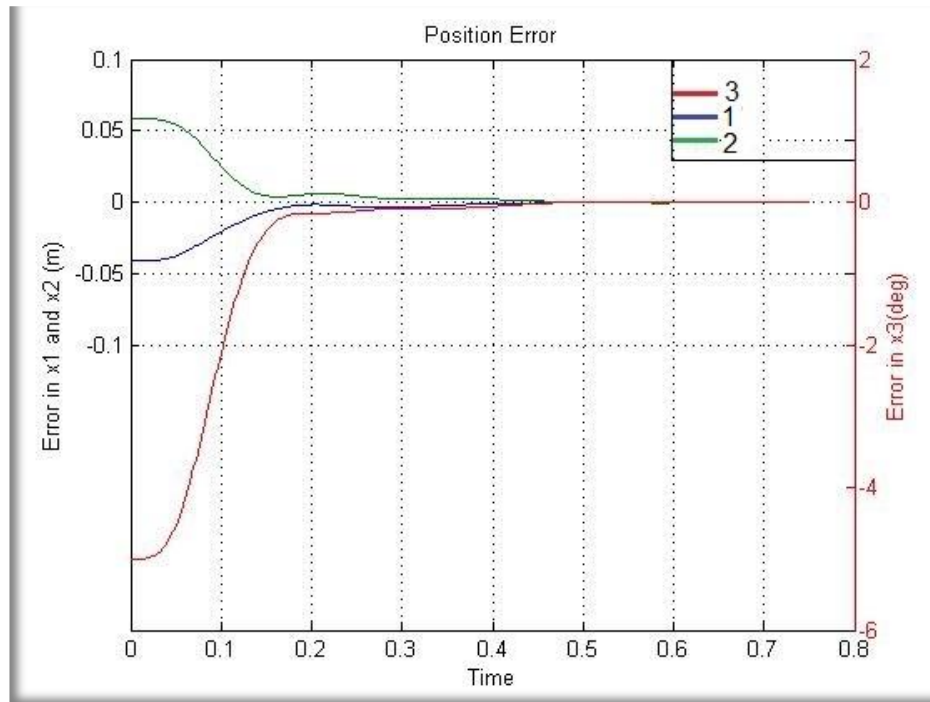


Figure 18 Position Errors (Second Group $\omega_i = 30 \text{ rad/s}$)

Third Group of Simulations

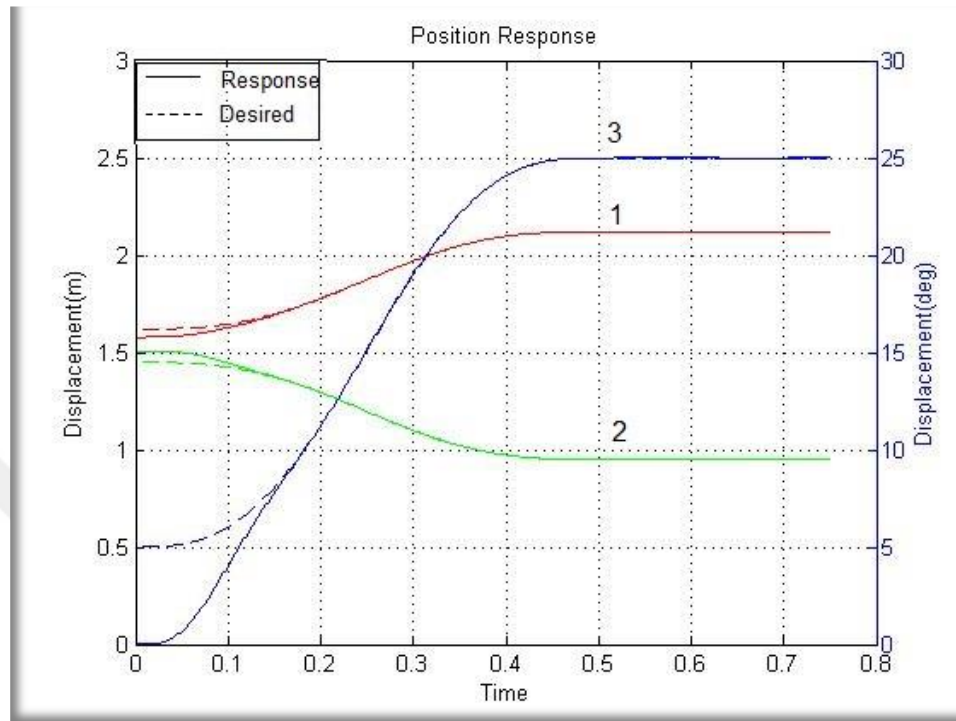


Figure 19 Position Response 1. x_1 , 2. x_2 , 3. x_3 (Third Group $\omega_i = 20 \text{ rad/s}$)

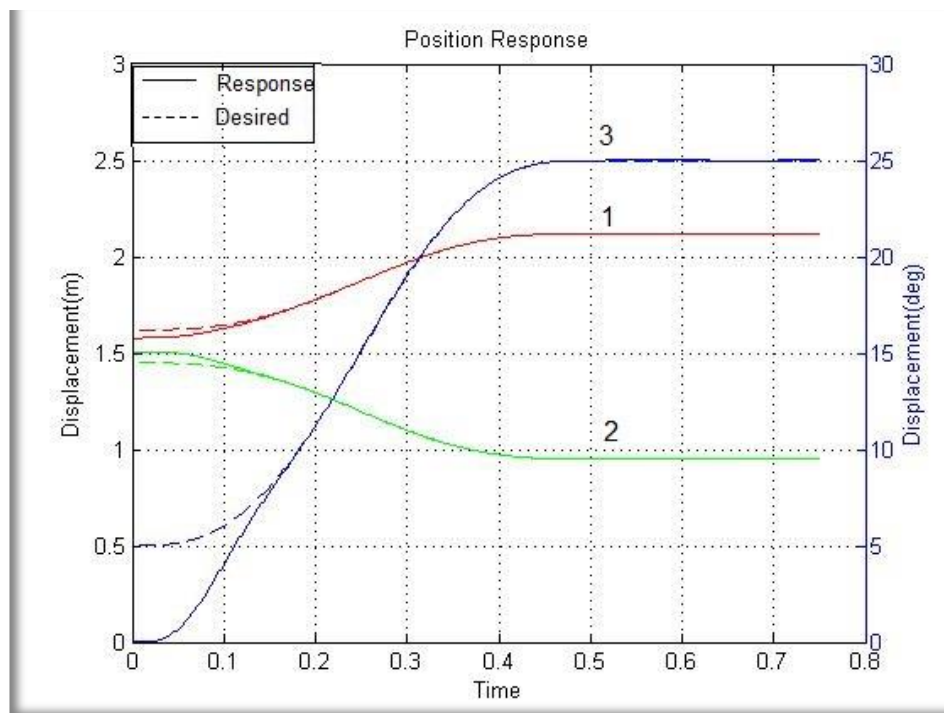


Figure 20 Position Response 1. x_1 , 2. x_2 , 3. x_3 (Third Group $\omega_i = 30 \text{ rad/s}$)

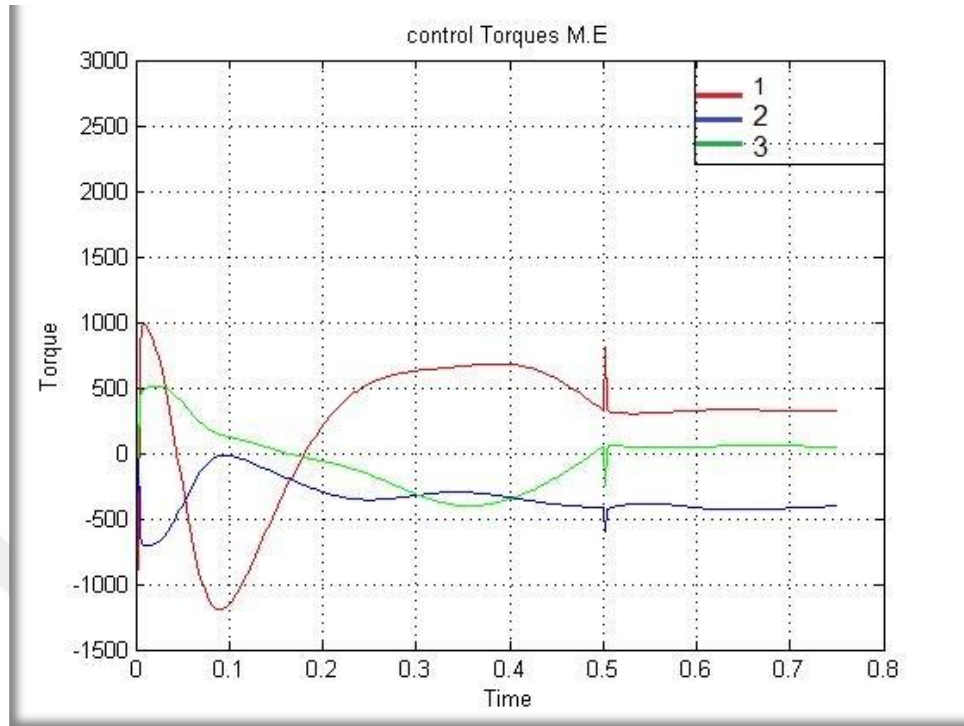


Figure 21 Control Torques 1. T_1^a , 2. T_2^a , 3. T_3^a (Third Group $\omega_i = 20 \text{ rad/s}$)

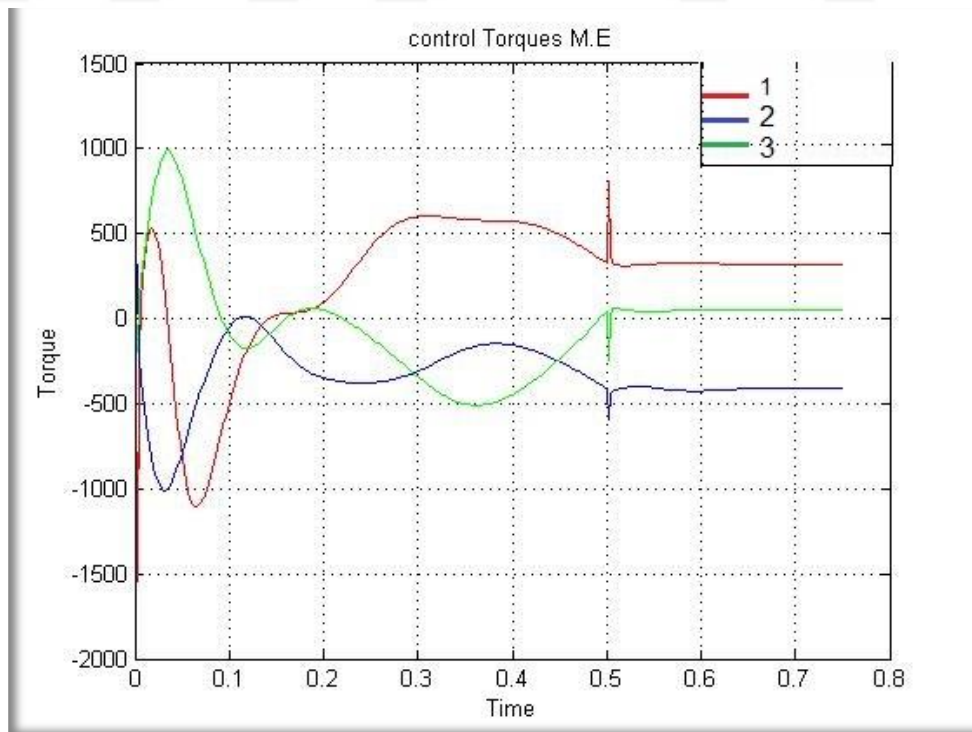


Figure 22 Control Torques 1. T_1^a , 2. T_2^a , 3. T_3^a (Third Group $\omega_i = 30 \text{ rad/s}$)

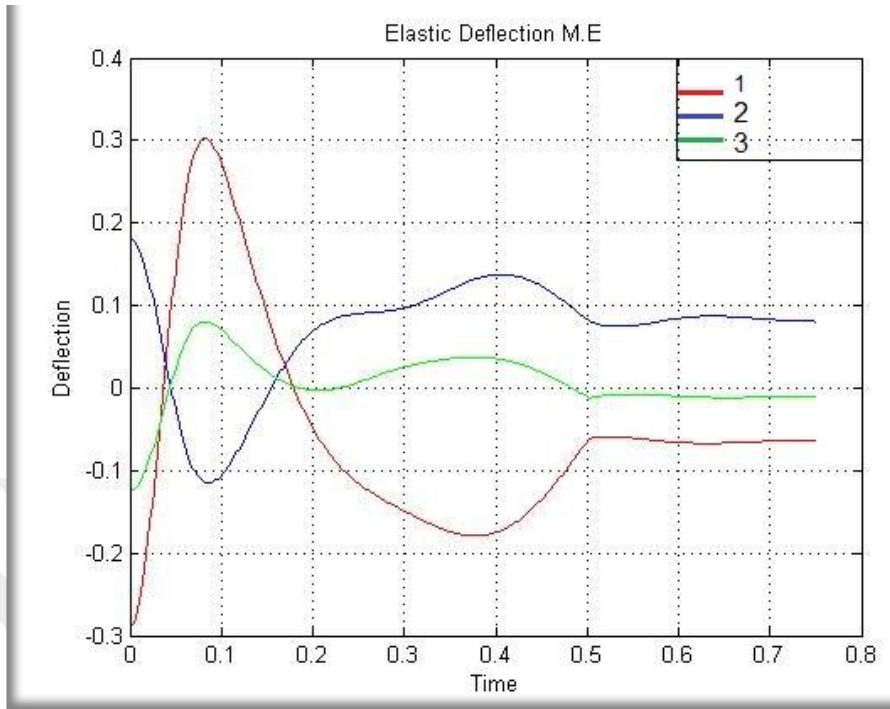


Figure 23 Deflections 1. $\theta_1 - \phi_1$, 2. $\theta_2 - \phi_2$, 3. $\theta_3 - \phi_3$ (Third Group $\omega_i = 20\text{rad/s}$)

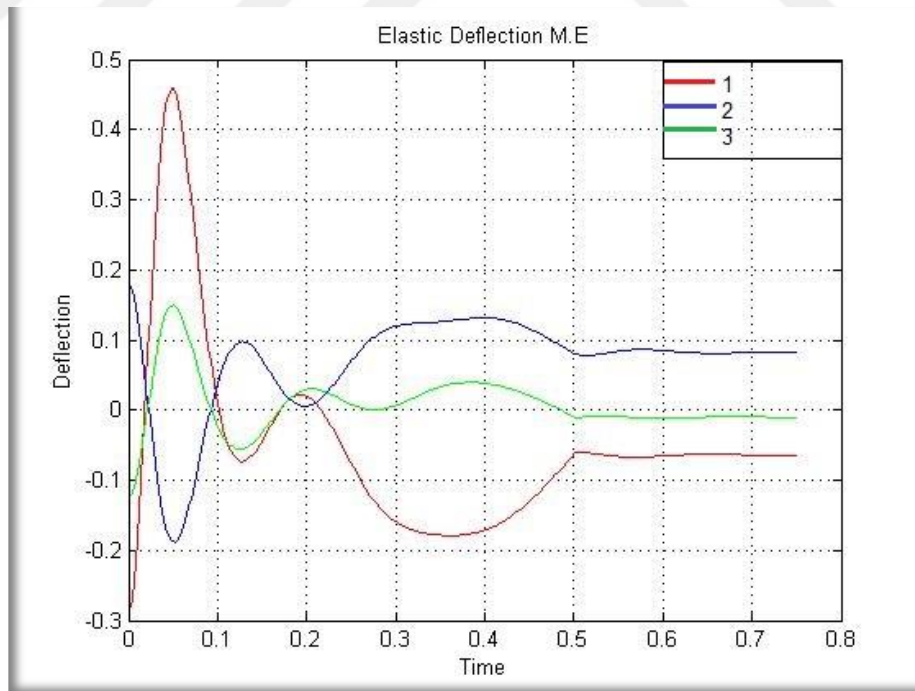


Figure 24 Deflections 1. $\theta_1 - \phi_1$, 2. $\theta_2 - \phi_2$, 3. $\theta_3 - \phi_3$ (Third Group $\omega_i = 30\text{rad/s}$)

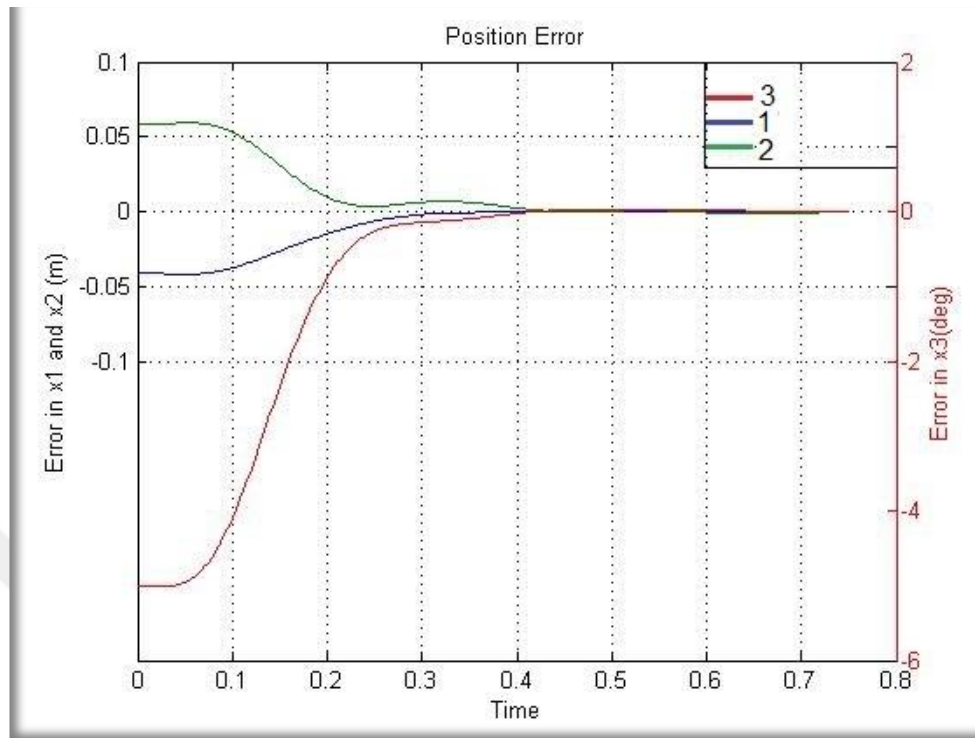


Figure 25 Position Errors (Third Group $\omega_i = 20 \text{ rad/s}$)

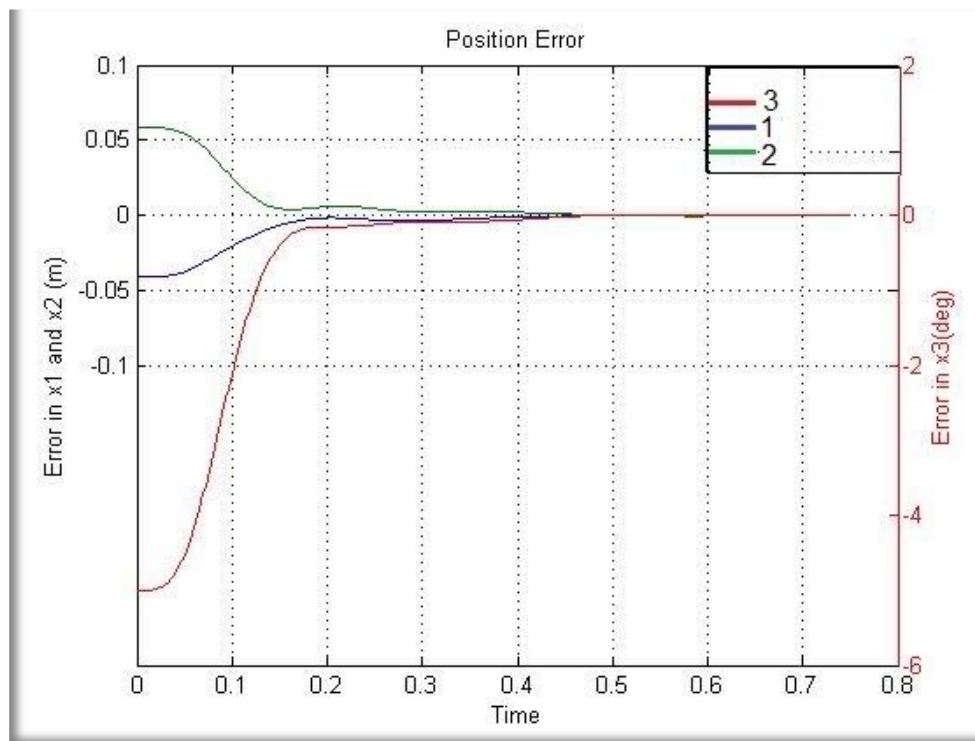


Figure 26 Position Errors (Third Group $\omega_i = 30 \text{ rad/s}$)

CHAPTER 4

DISCUSSIONS AND CONCLUSION

4.1 Discussions

The simulations are executed for two independent groups with the same feedback gain constants. The first group is simulated without regarding modeling errors while the second group will be simulated by considering modeling errors. In both of the groups and while taking initial position error into consideration, it is noticed that good tracing performances are reached for motion tracking. Then again, it is observed that initial errors in position lead to large initial control torques and large initial elastic deflections.

Because of the gravitational forces, none of the initial and final elastic deflections will be zero.

Each group is simulated under the determinant of initial position errors, while, the second group is simulated under the consideration of modeling errors as well as the initial position errors. For this issue, mass/inertia parameters and spring constant are assumed to be 20% smaller in the model. No notable change is noticed in tracking elastic deflections, errors and control torques. The control torques are increased (as observed also by the previous studies) at the discontinuities of the reference motion trajectories.

4.2 Conclusion

This thesis granted the motion trajectory tracking control law of flexible joint parallel robots use as a basis on solving the singular acceleration level inverse dynamic equations. By using the proposed method, further differentiations of task equations, constraint equations and equations of motion are avoided. This eases the calculations and makes the complexity less in equations. Actuator rotor and joint positions and velocities are the feedback variables only. Since it is only motion tracking control problem, contact forces are not existed though. The important thing about the algorithm is that any jump in z, \dot{z}, Γ and $\dot{\Gamma}$ requires infinitely large input control torques because they cannot make an instant effect on the end-effector accelerations and jerks. To avoid this z, \dot{z}, Γ and $\dot{\Gamma}$ are matched at the discontinuities of the reference motion trajectories by selecting the appropriate integration constants.

Simulations are executed for two groups with the same feedback gain constants but the first group is without regarding modeling errors and the second group is with regarding modeling errors. As a result, there will be good tracking properties for motion trajectories by using the proposed control algorithm.

In this thesis the motor dynamics is regardless so as to focus on the dynamics of the flexible joint manipulator. As a result it is assumed that the required control torques are utilized without notable delay. This assumption is satisfied if brushless DC motors are utilized that are widely used in manipulator applications. The frequency response of the current loop in brushless DC motors is wide enough for reducing any effect on outer control loops and though the motor dynamics can be disregarded.

REFERENCES

- [1] **İder K., (2005)**, “Inverse Dynamics of Parallel Manipulators in the Presence of Drive Singularities”, *Mechanism and Machine Theory*, Vol. 40, pp. 33-44.
- [2] **Spong M. W., (1987)**, “Modeling and Control of Elastic Joint Robots”, *Journal of Dynamic Systems, Measurement and Control*, Vol. 109, pp. 310-319.
- [3] **Jankowski K. P., Van Brussel H., (1992)**, “An Approach to Discrete Inverse Dynamics Control of Flexible Joint Robots”, *IEEE Transactions on Robotics and Automation*, No.5, Vol. 8, pp. 651-658.
- [4] **Forrest-Barlach M. G., Babcock S. M., (1987)**, “Inverse Dynamics Position Control of a Compliant Manipulator”, *IEEE Journal of Robotics and Automation*, No.1, Vol. Ra-3, pp. 75-83.
- [5] **İder K. and Özgören K., (2000)**, “Trajectory Tracking Control of Flexible Joint Robots”, *Computers and Structures*, Vol. 76, pp. 757-763.
- [6] **Dado M. H., Al-Huniti N. S., and Eljabali A. K., (2001)**, “Dynamic Simulation Model for Mixed-loop Planar Robots with Flexible Joint Drives”, *Mechanism and Machine Theory*, Vol. 36, pp. 547-559.
- [7] **Damien Chablat, Philippe Wenger, (2003)** “The Kinematic Analysis of a Symmetrical Three-Degree-of-Freedom Planar Parallel Manipulator”, *Institut de Recherche en Communications et Cybernétique de Nantes* 1, rue de la Noë, 44321 Nantes, France.
- [8] **İder K., Korkmaz O.,** “Trajectory tracking control of parallel robots in the presence of joint drive flexibility”, *Journal of Sound and Vibration* 319 (2009) pp. 77-90.
- [9] **Rivin E. I., (1984)**, “Compliance Breakdown for Robot Structures”, *Proceedings of the Symposium Engineering Applied Mechanics*, Toronto.
- [10] **The Mathworks Inc., (2012)**, “Matlab User's Guide”.

APPENDECIES A
CURRICULUM VIATE

PERSONAL INFORMATION

Surname, Name: ABDALJAWAD, Harith
Date and Place of Birth: 11 June 1986, Iraq
Marital Status: Single
Phone: +905364464484
Email: harith.mahdi1986@gmail.com

EDUCATION

Degree	Institution	Year of Graduation
M.Sc.	Çankaya Univ., Mechanical Engineering	2016
B.Sc.	Najaf Technical College	2011
High School	Private Arı High School	2005

WORK EXPERIENCE

Year	Place	Enrollment
2011-2012	Copperchase-Fourth Dimension Instructions	Site Engineer
2011-2012	Copper chase-Fourth Dimension Instructions	Draftsman
2011	Iraqi A.G.C	Marketing

FOREIN LANGUAGES

Advanced English, Average Turkish

HOBBIES

Football, Running, Translation, Poetry